FINAL REPORT

Ultrahigh-Resolution Fourier-Transform Ion Cyclotron Resonance Mass Spectrometry for Fingerprinting, Source Tracking, and Allocation of Per- and Polyfluoroalkyl Substances (PFASs)

SERDP Project ER20-1265

JULY 2021

Jens Blotevogel
Colorado State University

Nasim Pica
CDM Smith (formerly Colorado State University)

Amy McKenna
National High Magnetic Field Laboratory

John Kornuc
Naval Facilities Engineering and Expeditionary Warfare Center

SERDP
DOD ▪ EPA ▪ DOE

REPORT DOCUMENTATION PAGE

Form Approved
OMB No. 0704-0188

1. REPORT DATE *(DD-MM-YYYY)*	**2. REPORT TYPE**	**3. DATES COVERED** *(From - To)*
21/07/2021	SERDP Final Report	11/12/2019 - 12/12/2021

4. TITLE AND SUBTITLE

Ultrahigh-Resolution Fourier-Transform Ion Cyclotron Resonance Mass Spectrometry for Fingerprinting, Source Tracking, and Allocation of Per- and Polyfluoroalkyl Substances (PFASs)

5a. CONTRACT NUMBER
20-P-0008

5b. GRANT NUMBER

5c. PROGRAM ELEMENT NUMBER

6. AUTHOR(S)
Jens Blotevogel, Colorado State University

Nasim Pica, CDM Smith (formerly Colorado State University)

Amy McKenna, National High Magnetic Field Laboratory

John Kornuc, Naval Facilities Engineering and Expeditionary Warfare Center

5d. PROJECT NUMBER
ER20-1265

5e. TASK NUMBER

5f. WORK UNIT NUMBER

7. PERFORMING ORGANIZATION NAME(S) AND ADDRESS(ES)
Colorado State University
Civil and Environmental Engineering
1320 Campus Delivery
Fort Collins, CO 80523

8. PERFORMING ORGANIZATION REPORT NUMBER
ER20-1265

9. SPONSORING/MONITORING AGENCY NAME(S) AND ADDRESS(ES)
Strategic Environmental Research and Development Program (SERDP)
4800 Mark Center Drive, Suite 16F16
Alexandria, VA 22350-3605

10. SPONSOR/MONITOR'S ACRONYM(S)
SERDP

11. SPONSOR/MONITOR'S REPORT NUMBER(S)
ER20-1265

12. DISTRIBUTION/AVAILABILITY STATEMENT
DISTRIBUTION STATEMENT A. Approved for public release: distribution unlimited.

13. SUPPLEMENTARY NOTES

14. ABSTRACT
The widespread use of aqueous film-forming foams (AFFFs) for hydrocarbon fuel firefighting has created an environmental legacy for the U.S. Department of Defense (DoD) as per- and polyfluoroalkyl substances (PFASs) continue to cause sustained groundwater plume development. However, PFASs have been widely used in industrial and consumer products due to heat, oil and water resistance, and PFASs leaching from landfills, wastewater treatment plants (WWTPs) and other sources may lead to co-located plume development. The overarching objective of this Limited Scope Project was to apply ultrahigh-resolution Fourier-Transform Ion Cyclotron Resonance Mass Spectrometry (FT-ICR MS) to identify compounds in AFFFs at the molecular level that can be used to guide the development of novel analytical approaches to identify unique marker compounds for AFFF “fingerprinting” and PFAS source allocation, and catalogue PFASs associated with AFFF releases.

15. SUBJECT TERMS
PFAS, environmental forensics, AFFF, groundwater, wastewater, precursors, high-resolution mass spectrometry, suspect screening, non-target analysis, FT-ICR MS, source allocation, source tracking, plume dating, fingerprinting

16. SECURITY CLASSIFICATION OF:			**17. LIMITATION OF ABSTRACT**	**18. NUMBER OF PAGES**	**19a. NAME OF RESPONSIBLE PERSON**
a. REPORT	**b. ABSTRACT**	**c. THIS PAGE**			Jens Blotevogel
UNCLASS	UNCLASS	UNCLASS	UNCLASS	64	**19b. TELEPHONE NUMBER** *(Include area code)* 970-491-8880

TABLE OF CONTENTS

LIST OF FIGURES

LIST OF TABLES

LIST OF ACRONYMS

AFB – Air Force Base

AFFF – Aqueous film-forming foam

AOP – Advanced oxidation process

APPI – Atmospheric pressure photoionization

CSU – Colorado State University

DBE – Double bond equivalents

DoD – Department of Defense

DOM – Dissolved organic matter

DPS – Dehydrated paper sludge

ECF – Electrochemical fluorination

ESI – Electrospray ionization

FT-ICR – Fourier-transform ion cyclotron resonance

FTOH – Fluorotelomer alcohol

HDPE – High-density polyethylene

HFPO – Hexafluoropropylene oxide

HPLC – High-pressure/performance liquid chromatography

IUPAC – International Union of Pure and Applied Chemistry

KGS – KOMAN Government Solutions

KMD – Kendrick mass defect

LC – Liquid chromatography

LLE – Liquid-liquid extraction

MS – Mass spectrometry or mass spectrometer

NHMFL – National High Magnetic Field Laboratory

NOSC – Nominal oxidation state of carbon

OECD – Organisation for Economic Co-operation and Development

PAP – Polyfluoroalkyl phosphate ester

PCA – Principal component analysis

PFAA – Perfluoroalkyl acid

PFAS – Per- and polyfluoroalkyl substance

PFCA – Perfluoroalkyl carboxylic acid

PFHxS – Perfluorohexane sulfonic acid

PFOA – Perfluorooctanoic acid

PFOS – Perfluorooctane sulfonic acid

PFSA – Perfluoroalkane sulfonic acid

QA – Quality assurance

QC – Quality control

QQQ – Triple quadrupole

QTOF – Quadrupole time-of-flight

RF – Radio frequency

RPM – Remedial program manager

SERDP – Strategic Environmental Research and Development Program

SRC – Shredded recycled cardboard

UME – UltraMassExplorer

VKD – van Krevelen diagram

VOA – Volatile organic analysis

WAX – Weak anion exchange

WCX – Weak cation exchange

WWTP – Wastewater treatment plant

KEYWORDS

PFAS, environmental forensics, AFFF, groundwater, wastewater, precursors, high-resolution mass spectrometry, suspect screening, non-target analysis, FT-ICR MS, source allocation, source tracking, plume dating, fingerprinting

ACKNOWLEDGEMENTS

The authors thank Dr. Hamidreza Sharifan (formerly CSU), Dr. Robert Young (formerly CSU), Dr. Huan Chen (NHMFL), Sydney Niles (NHMFL), Sharon Stone (Peterson AFB), Dr. Andrea Hanson (CSU) Dr. Gregory Dooley (CSU), and Brian Cranmer (CSU) for their invaluable contributions and input. Furthermore, the authors thank Dr. Christopher Higgins and his team at the Colorado School of Mines for generously providing an extensive PFAS suspect screening list.

A portion of this work was performed at the National High Magnetic Field Laboratory ICR User Facility, which is supported by the National Science Foundation Division of Chemistry and Division of Materials Research through DMR-1644779 and the State of Florida.

ABSTRACT

Introduction and Objectives

The widespread use of aqueous film-forming foams (AFFFs) for hydrocarbon fuel firefighting has created an environmental legacy for the U.S. Department of Defense (DoD) as per- and polyfluoroalkyl substances (PFASs) continue to cause sustained groundwater plume development. However, PFASs have been widely used in industrial and consumer products due to heat, oil and water resistance, and PFASs leaching from landfills, wastewater treatment plants (WWTPs) and other sources may lead to co-located plume development. The overarching objective of this Limited Scope Project was to apply ultrahigh-resolution Fourier-Transform Ion Cyclotron Resonance Mass Spectrometry (FT-ICR MS) to identify compounds in AFFFs at the molecular level that can be used to guide the development of novel analytical approaches to identify unique marker compounds for AFFF "fingerprinting" and PFAS source allocation, and catalogue PFASs associated with AFFF releases.

Technical Approach

Groundwater, WWTP effluent, and AFFF samples were collected at three DoD sites. The samples were liquid-liquid extracted and analyzed by ultrahigh-resolution FT-ICR MS on the world's highest performing mass spectrometer (21 tesla) at the National High Magnetic Field Laboratory. A workflow was developed to assign elemental compositions for fluorinated compounds at four Confidence Levels. Data and dimensionality reduction techniques were used to fingerprint the sample composition and to develop forensic analysis approaches.

Results

First, we discovered 300 new PFAS species and 75 novel PFAS classes that were unambiguously identified at <0.2 ppm mass error and based on being members of CF_2 Kendrick mass defect (KMD) series. Thousands of additional PFASs were detected at varying confidence levels. Second, we demonstrated how sample fingerprinting approaches reveal compositional differences between samples. Third, our forensic analysis was able to discriminate between different samples and sources based on compositional variability. Fourth, we highlight PFASs that are unique to specific sources. These analytes can potentially be used as source-specific marker compounds after future confirmation and validation on other mass spectrometric instruments.

Benefits

FT-ICR MS achieves the highest mass resolving power and mass accuracy, far surpassing quadrupole time-of-flight (QTOF) and Orbitrap MS systems, sufficient to identify and resolve PFAS compounds without prior chromatographic separation. Consequently, FT-ICR MS can reveal complex sample composition and molecular features that would remain unresolved on lower-performance instruments. This first-of-its-kind application of FT-ICR MS and the workflow developed here are a critical first step in cataloguing PFASs associated with AFFF and non-AFFF sources as well as in identifying unique marker compounds for fingerprinting that can be targeted in the future on more widely accessible mass spectrometric instruments. Ultimately, this information will provide critical guidance to DoD remedial program managers (1) to track transformation and retardation processes of AFFFs, (2) to date plumes, (3) to understand the extent of PFAS contamination, and (4) to determine the potential liability associated with past releases.

EXECUTIVE SUMMARY

Introduction

Per- and polyfluoroalkyl substances (PFASs) are active ingredients of aqueous film-forming foams (AFFFs). Due to the unique physicochemical properties of PFASs, their applications are also widespread in agricultural, industrial, commercial, and consumer products. Consequently, source zone allocation in PFAS-impacted groundwater is challenging. Efforts in tracking PFAS sources have usually centered on linking specific PFASs to a particular formulation. The sensitive quantification of PFASs in aqueous samples is typically achieved by liquid chromatography coupled with tandem or triple quadrupole (QQQ) mass spectrometry (MS). High-resolution mass spectrometers such as quadrupole time-of-flight (QTOF) and Orbitrap can be used to identify unknown PFASs. However, with increasing analyte molecular weight or mass-to-charge ratio *m/z*, an increasing number of molecular formulas arise, challenging analyte identification.

Within scientific fields such petroleum hydrocarbon and natural organic matter research, Fourier-transform ion cyclotron resonance mass spectrometry (FT-ICR MS) has become the method of choice for complex mixture analysis. The power of this technique lies in the ability to resolve compounds that differ in mass by roughly the mass of an electron while simultaneously detecting tens of thousands of compounds. However, FT-ICR MS analysis has not yet been applied for the analysis of PFAS-impacted media. Consequently, as FT-ICR MS is uniquely capable of identifying organic species and mixture signatures in complex media at both resolution and accuracy unmatched by any other mass spectrometric technique, its potential to serve as a forensic tool for PFASs needs to be developed and explored.

Objectives

The objectives of this Limited Scope Project were to apply ultrahigh-resolution FT-ICR MS (1) to develop code, workflow, and data reduction techniques for the identification of PFASs in AFFF and complex environmental samples at unmatched resolution, (2) to fingerprint PFAS composition in environmental samples and identify marker compounds for source tracking, and (3) to create a database of identified PFASs specific to AFFF and non-AFFF releases.

To meet our research objectives, the following hypotheses were tested:

1) FT-ICR MS can identify and characterize PFASs (and relevant non-fluorinated compounds) without interference in complex mixtures such as AFFFs at a mass resolution unmatched by other high-resolution mass spectrometric methods (QTOF, Orbitrap), leading to the discovery of yet unknown PFAS species.
2) Comparison among different PFAS-containing samples/sources will reveal product-specific markers.
3) Novel data analysis techniques can be used for sample fingerprinting, which will ultimately assist with source tracking, dating, and allocation of PFAS plumes.

Technical Approach

Fourier-transform ion cyclotron resonance mass spectrometry (FT-ICR MS) is an emerging analytical approach that offers the highest mass resolution and mass accuracy currently achievable. It can be paired with different selective ionization modes to target specific functional groups. The ultrahigh resolving power of FT-ICR MS has advanced the field of "petroleomics", i.e., the characterization of petroleum at the molecular level, and therefore enabled the direct characterization of complex organic sample mixtures without prior fractionation (Rodgers et al. 2005). At a mass range of about 50-1500 Da, it can measure mass-to-charge ratios with sub-ppm error.

Figure ES 1: 21 tesla FT-ICR MS at the National High Magnetic Field Laboratory (NHMFL).

Groundwater, wastewater treatment plant (WWTP) effluent, and AFFF samples were collected at three U.S. DoD sites (Sites A, B, and C in this report). The samples were liquid-liquid extracted and analyzed by ultrahigh-resolution FT-ICR MS on the world's highest performing mass spectrometer (21 tesla) at the National High Magnetic Field Laboratory (Figure ES 1; Hendrickson et al. 2015, Smith et al. 2018).

Results and Discussion

Tens of thousands of analyte peaks were detected by FT-ICR MS in the collected samples. To develop a workflow of robust rules for the identification of PFASs in the collected spectra, statistical analyses of two databases with known PFASs was conducted. The first database was compiled by the Organisation for Economic Co-operation and Development that contains 4730 species (OECD 2021). The second database was a list of 2154 species generously provided to us by Dr. Christopher Higgins at the Colorado School of Mines.

As a first step after spectral calibration and elimination of peaks with a signal-to-noise ratio of <6, all spectra were processed with PetroOrg® for the identification of and subsequent elimination of DOM species. Next, a suspect screening for known PFASs listed in the two databases was conducted. Matches of computed neutral masses were limited to a ppm error <0.2 and validated by presence and correct isotope abundances. PFASs identified as "knowns" during suspect screening were assigned a Confidence Level 1. For the remaining peaks not identified as PFASs during suspect screening, a non-targeted analysis was conducted to identify "unknowns". First, a theoretical PFAS library was developed in which exact masses for a variety of element and isotope compositions was calculated for matching with detected *m/z* values. The library was integrated into UltraMassExplorer. Subsequently, several rigorous steps were taken to further restrict the

number of assigned formulas in order to assign one unique formula with the highest possible level of confidence at a ppm mass error of <0.2. Members of CF_2 Kendrick mass defect (KMD) series were finally identified to verify consistent assignments CF_2 KMD series members with an unambiguous assigned molecular formula were identified as **Level 2** PFAS. Members of CF_2 KMD series with ambiguous molecular formulas were assigned an unambiguous formula from matching with their identified CF_2 KMD series and classified as **Level 3** PFAS. For unknown species which were not a member of a CF_2 KMD series, a more stringent ppm error range of <0.1 was applied. After this final step, species with one unambiguous assignment were classified as **Level 4** PFAS, while species with ambiguous assignments were left unidentified.

At all confidence levels combined, thousands of previously unreported PFASs and 75 novel PFAS classes were detected in the collected samples. All detected species were compiled in a mass spectral library that is submitted along with this report and that may serve as a molecular catalogue to accelerate future PFAS identification and AFFF fingerprinting. For brevity, we are focusing the discussion here on one electrochemical fluorination AFFF sample as well as a groundwater sample and WWTP effluent sample collected at the same site. Furthermore, our data analysis will only include known and unknown PFASs identified at the highest Confidence Levels 1 and 2, although all detections are included in the mass spectral library to enable future mining efforts.

For sample fingerprinting, we developed modified van Krevelen diagrams (VKDs, Figure ES 2), where each dot in the diagram represents one identified species. For example, perfluorohexane sulfonic acid (PFHxS, $C_6HF_{13}O_3S$) has an F/C ratio of 13/6 = 2.17 and an O/C ratio of 3/6 = 0.50. Furthermore, the nominal oxidation state of carbon (NOSC), originally defined for natural organic matter, was adjusted for PFASs and plotted against molecular weight (i.e., *m/z*). In all three samples, perfluoroalkane sulfonic acids (PFSAs) were the dominant perfluoroalkyl acids (PFAAs), while the abundance of perfluoroalkyl carboxylic acid (PFCAs) was relatively low. However, the three samples showed distinct variability in their precursor composition. Compared to the original AFFF sample, the PFASs in the AFFF-impacted groundwater revealed an overall higher degree of oxidation while having a lower molecular weight, likely because of precursor transformation and retardation processes along the groundwater flow path. The WWTP sample was dominated by precursors with high degree of hydrogenation and low degrees of both oxygenation and fluorination.

For forensic analysis, principal component analysis (PCA) was conducted (Figure ES 3). A clear separation of the AFFF sample from all other samples was observed. While all Site A samples were clustered together, there was a clear separation between the groundwater and the WWTP samples from Site B as well as between the two groundwater samples from Site C along the second principal component. When PCA was performed on the Site A samples only, the groundwater samples collected offbase and upgradient of the site were clearly clustered and separated compared to the two onbase samples. These separations indicate impacts from different PFAS sources.

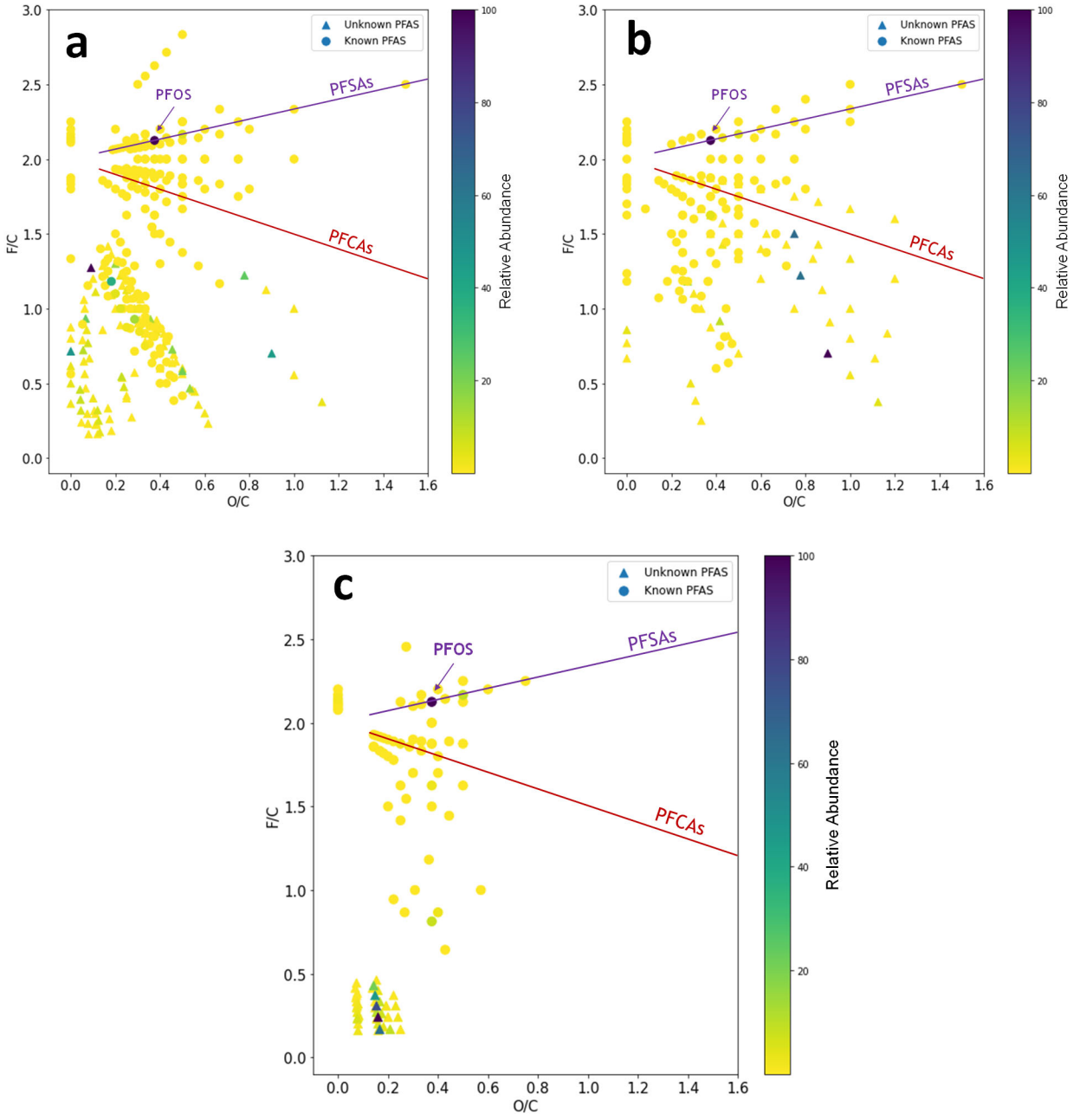

Figure ES 2: Modified van Krevelen diagrams illustrating the PFASs detected at Confidence Levels 1 (Known PFAS) and 2 (Unknown PFAS) in (a) the AFFF sample, (b) the groundwater sample from Site B, and (c) the WWTP effluent sample from Site B. The lines on which PFSAs and PFCAs fall are highlighted.

Finally, a strategy for the identification of marker compounds was developed by separating the molecular formulas identified at Confidence Levels 1 and 2 is into common and unique PFAS species (Figure ES 3). A total of 64 unique PFASs were identified in the WWTP effluent sample (22 known and 42 unknown PFASs) that were absent in the AFFF and groundwater samples. For an ultimate identification of source-specific marker compounds, a greater number of samples will have to be analyzed in the future to increase confidence in their uniqueness.

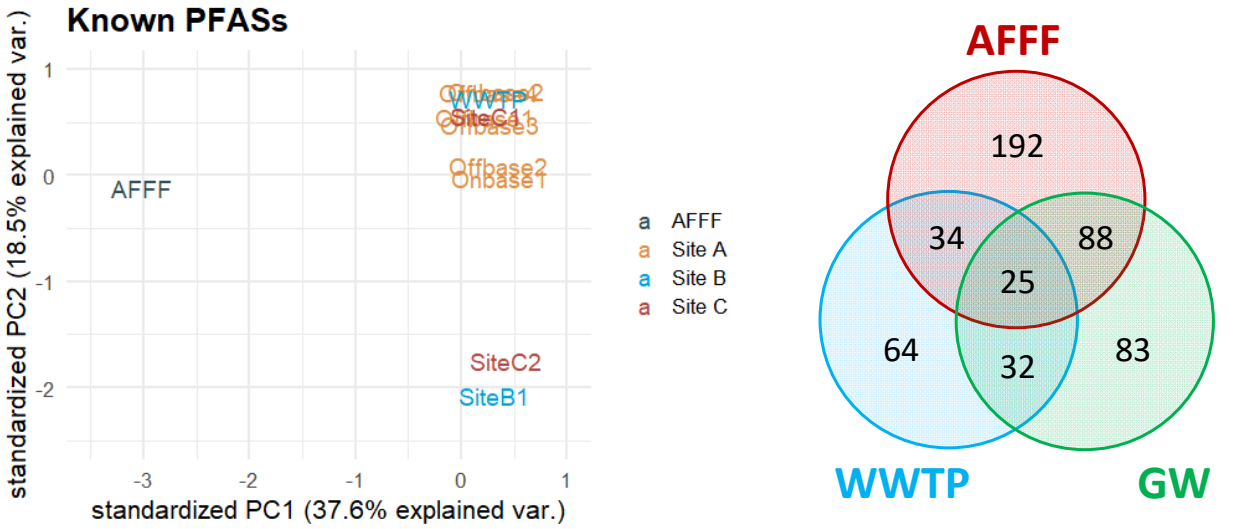

Figure ES 3: Left: Principal component analysis for all analyzed samples based on PFASs identified at Confidence Level 1. Right: Venn diagrams for total PFASs identified at Confidence Levels 1 and 2 in the AFFF, Site B 1 groundwater, and WWTP effluent samples, illustrating common and unique species.

Implications for Future Research and Benefits

The developmental work performed in this one-year limited scope project clearly demonstrates the unmatched capabilities of FT-ICR MS for the identification of complex PFAS mixtures via ultrahigh mass resolving power and mass accuracy, revealing molecular features that would remain unresolved on lower-performance instruments. Here, we discovered 300 new PFAS species and 75 novel classes at the highest confidence levels, and demonstrated how these data can be used in the future for PFAS identification, sample fingerprinting, forensic analysis, and identification of source-specific marker compounds.

While this work is a major advancement in the identification of PFASs and forensic analysis, several tasks remain to be performed in order to take full advantage of the instrument's full capabilities:

1) As shown in Table 1, thousands of peaks remain unassigned, neither being identified as DOM by PetroOrg® nor as PFASs through our spectral processing. While some of these peaks may be fragments, isotopologues, or background contamination, it is certainly possible that some PFASs did not pass our stringent identification criteria such as ±0.1 ppm mass error.

2) Our analyses in this report focus on species ionizable in negative ESI. Additional steps for processing positive-ion spectra will need to be developed and are challenged by the occurrence of multiple adducts (i.e., protonated, ammoniated, sodiated, etc.). For groundwater forensics, negative ESI may be sufficient as negatively charged species typically dominate the PFAS composition in a downgradient plume. However, for tasks such as AFFF characterization or soil analysis, the development of a positive ESI workflow would be valuable.

3) Even though a low ppm mass error was achieved for known PFASs, a larger number of commercially available PFAS standards (or "reference material") would be helpful for the calibration of PFAS spectra (Savory et al. 2011).

4) To add further lines of evidence, and thus confidence, to our formula assignments, MSn fragmentation and possibly chromatographic separation may be attempted in future experiments.

5) The source of PFAS detections in the blanks, though at very low abundances, needs to be addressed. Likely, specific instrument cleaning protocols need to be developed for the analysis of PFAS samples.

6) To expand our mass spectral library, more samples need to be analyzed, especially AFFF products and common alternative PFAS sources such as WWTP effluent and landfill leachate. A larger, more representative database for each of these sources will enable the identification of source-specific marker compounds and improve sample fingerprinting. Furthermore, groundwater sampling at higher spatial resolution and along a known direction of groundwater flow will enable more accurate conclusions regarding source allocation.

7) Newly discovered PFASs should be validated through additional QTOF or Orbitrap analyses including chromatographic separation and fragmentation.

8) Ultimately, the analysis of identified product- or source-specific marker compounds needs to be transferred to more accessible, commercial LC/MS-MS systems.

Collectively, this first-of-its-kind application of FT-ICR MS and the workflow developed here are a critical first step in cataloguing PFASs associated with AFFF and non-AFFF sources as well as in identifying unique marker compounds for fingerprinting that can be targeted in the future on more widely accessible mass spectrometric instruments. Ultimately, this information will provide critical guidance to DoD remedial program managers (1) to track transformation and retardation processes of AFFFs, (2) to date plumes, (3) to understand the extent of PFAS contamination, and (4) to determine the potential liability associated with past releases.

1 OBJECTIVE

The widespread use of aqueous film-forming foams (AFFFs) for fighting hydrocarbon fuel fires has created an environmental legacy for the U.S. DoD. Besides being key components of AFFFs for firefighting, per- and polyfluoroalkyl substances (PFASs) are widely used in industrial and consumer products (Tokranov et al. 2019, Wang et al. 2017). The leaching of PFASs from landfills, wastewater treatment plants (WWTPs) and other sources has been widely documented (Lang et al. 2016, Schultz et al. 2006). PFAS plumes from different sources may co-locate with time (Figure 1). Thus, there is a critical need to differentiate DoD and non-DoD sources to help Remedial Program Managers (RPMs) at the DoD determine both the nature and extent of DoD-related PFAS contamination as well as potential associated liabilities.

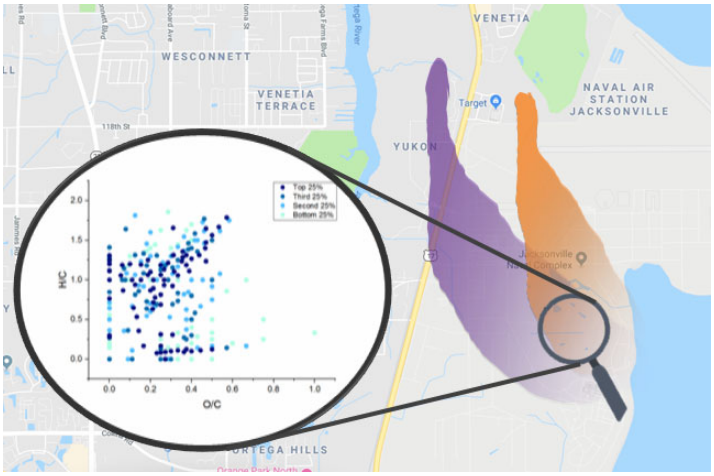

Figure 1: Conceptual overview of this Limited Scope Project. Ultrahigh-resolution FT-ICR MS will be used in combination with novel data analysis approaches for PFAS compositional fingerprinting.

Fourier-transform ion cyclotron resonance mass spectrometry (FT-ICR MS) (Marshall et al. 1998) has become the method of choice for complex mixture analysis (Smith et al. 2018) due to high mass-resolving power, high mass accuracy, and dynamic range (ratio of highest to lowest peak) sufficient to resolve and assign elemental compositions to tens of thousands of compounds simultaneously (e.g., petroleum and dissolved organic matter). However, while successfully applied for petroleum hydrocarbon and natural organic matter mixtures, the unprecedented resolving power of FT-ICR MS has never been used for the analysis of organofluorine mixtures.

Consequently, the objectives of this Limited Scope Project were to apply ultrahigh-resolution FT-ICR MS (1) to develop code, workflow, and data reduction techniques for the identification of PFASs in AFFF and complex environmental samples at unmatched resolution, (2) to fingerprint PFAS composition in environmental samples and identify marker compounds for source tracking, and (3) to create a database of identified PFASs specific to AFFF and non-AFFF releases.

To meet our research objectives, the following hypotheses (**Hyp.**) were tested:

Hyp. 1 FT-ICR MS can identify and characterize PFASs (and relevant non-fluorinated compounds) without interference in complex mixtures such as AFFFs at a mass resolution unmatched by other high-resolution mass spectrometric methods (quadrupole time-of-flight (QTOF), Orbitrap), leading to the discovery of yet unknown PFAS species.

Hyp. 2 Comparison among different PFAS-containing samples/sources will reveal product-specific markers.

Hyp. 3 Novel data analysis techniques can be used for sample fingerprinting, which will ultimately assist with source tracking, dating, and allocation of PFAS plumes.

2 BACKGROUND

2.1 Introduction

Due to the unique physicochemical properties of PFASs, their applications are widespread in agricultural, industrial, commercial, and consumer settings (Figure 2; Sharifan et al. 2021). Because of these diverse PFAS applications coupled with their persistence in the environment, tracking their original source in environmental samples is challenging. Different PFASs and PFAS-containing products are formulated for various purposes, and affected water bodies and groundwater plumes may become commingled. A primary source of PFASs that directly contaminates the subsurface is the use of AFFF in fire-training areas at military bases or airports, which have shown long-term impacts on groundwater quality (Nickerson et al. 2020). However, many other non-AFFF sources exist as described below.

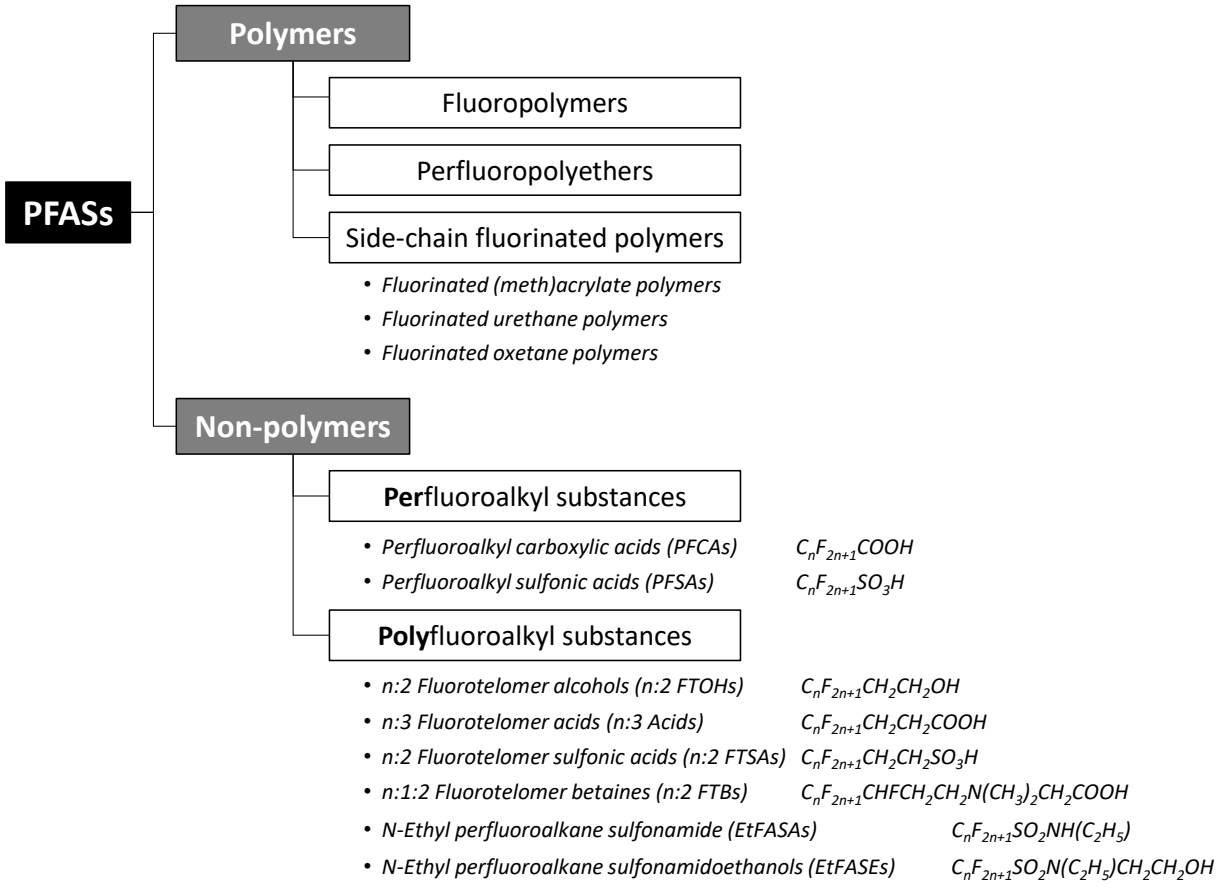

Figure 2: Classification of PFASs based on Buck et al. (2011).

Efforts in tracking PFAS sources have usually centered around linking specific PFASs to a particular formulation, using statistical and machine learning approaches (Kibbey et al. 2020; Hu et al. 2018; Rosenqvist et al. 2017). The sensitive quantification of PFASs in aqueous samples is typically achieved by liquid chromatography coupled with tandem or triple quadrupole (QQQ) mass spectrometry (MS). High-resolution mass spectrometers such as quadrupole time-of-flight

QTOF and Orbitrap can be used to identify unknown PFASs. With a resolving power on the order of tens to a few hundreds of thousand, these mass spectrometers identify compounds based on their accurate mass (in addition to their fragmentation pattern). Notable studies identifying a large range of previously unreported species are for instance the reports by D'Agostino & Mabury (2014), Mejia-Avendaño et al. (2017), and Barzon-Hanson et al. (2017), and several others exist. However, with increasing analyte molecular weight or mass-to-charge ratio *m/z*, an increasing number of molecular formulas arise that, accounting for the instrument- and method-specific ppm error, may match an observed accurate mass.

Within scientific fields such petroleum hydrocarbon and organic matter research, FT-ICR MS has become the method of choice for complex mixture analysis (Smith et al. 2018). The power of this technique lies in the ability to resolve compounds that differ in mass by roughly the mass of an electron while simultaneously detecting more than 80,000 compounds from the background hydrocarbon matrix (McKenna et al. 2014; Gueneli et al. 2018; Smith et al. 2018). However, while products such as electrochemical fluorination AFFFs are highly complex mixtures, FT-ICR MS analysis has not yet been applied for the analysis of PFAS-impacted media. Consequently, as FT-ICR MS is uniquely capable of identifying organic species and mixture signatures in complex media at both resolution and accuracy unmatched by any other mass spectrometric technique, its potential to serve as a forensic tool for PFASs needs to be developed and explored.

2.2 Common Sources and Signatures of PFAS Subsurface Contamination

2.2.1 Atmospheric Deposition

Atmospheric deposition of PFASs is an important contamination route of surface soils and water (Gottschall et al. 2017) that can create a regional "background" level in terrestrial ecosystems (Brusseau et al. 2020). In the atmosphere, PFASs are primarily transported by long-range forces, including the seasonal winds and unpredicted storms. Airborne PFASs originating from major sources such as manufacturing facilities and urban centers mainly comprise neutral volatile polyfluorinated compounds such as fluorotelomer alcohols (FTOHs), but also ionizable species, including perfluorooctanoic acid (PFOA) and perfluorooctane sulfonic acid (PFOS) (Ahrens et al. 2012; Barton et al. 2006; Piekarz et al. 2007; Yao et al. 2017). At reported lifetimes on the order of tens of days, polyfluorinated precursors undergo atmospheric oxidation to form PFAAs (Ellis et al. 2004; Piekarz et al. 2007; Ellis et al. 2003).

In worldwide reported data, collected soil samples contained a wide range of total PFCAs (∑PFCAs) from 29 to 14,300 pg g^{-1} (Rankin et al. 2016). The geometric mean value for the ubiquitous presence of ∑PFCAs was reported at 930 μg kg^{-1}, which was five times higher than its level in the southern hemisphere (Rankin et al. 2016). Similarly, the total perfluoroalkane sulfonic acids (∑PFSAs) of 170 μg kg^{-1} were approximately seven times greater than their level in the southern hemisphere (Rankin et al. 2016). In 2020, Galloway et al. documented that maximum PFAS concentrations may often be found within 20 km from the source towards wind direction (Galloway et al. 2020). The emission rate is a driving factor in the atmospheric deposition of PFASs. In a fluorochemical factory in China, the air emission rate of ΣPFASs was estimated 28 g $day^{-1,}$ which was remarkably low compared to its water discharge rate at 7000 g day^{-1} (Chen et al. 2018).

Likewise, previous findings demonstrated a strong correlation between historical data on PFOA and hexafluoropropylene oxide (HFPO) levels in environmental samples and the direction of the prevailing wind from a fluoropolymer factory in Ohio, USA (Galloway et al. 2020). In a non-target

mass analysis of widely distributed soil samples in New Jersey, highly identical PFASs ($\geq(CF_2)_7$) with distinct formulas and structures confirmed their potential airborne origin (Washington et al. 2020). Another study in Fuxin, China attested to strong effects of atmospheric deposition by observing a significant decline in soil concentrations at downwind direction of two fluoropolymer industrial facilities (Chen et al. 2018). However, the deposition rate of PFASs varied widely between reported data from wet and dry depositions. The fastest deposition rate was reported by 10^{-4} μg m^{-2} s^{-1} (Galloway et al. 2020), and the lowest rate was estimated at a dry deposition of 3 x 10^{-8} μg m^{-2} s^{-1} (Fang et al. 2018). The aerodynamic shape, size, and weight of the aerosols or dust is a critical factor that affects the PFAS deposition rate through the long-range forces. It is very difficult to characterize the aerosols containing the PFASs. For example, PFOS in the outdoor deposited dust around a manufacturing facility in Wuhan, China, reached up to 4300 μg g^{-1} (Wang et al. 2010), and perfluoroalkyl acids (PFAAs) in the collected dust was 9495 ng g^{-1} around the fluorochemical industrial park in Huantai, China (Su et al. 2016).

2.2.2 Aqueous Film-forming Foams

Aqueous film-forming foams are Class B firefighting foams used to extinguish hydrocarbon fuel fires. Besides water, they contain hydrocarbon surfactants, organic solvents, polymers, other additives, and up to >10% fluorosurfactants (ITRC 2020). PFOS, other PFSAs, and their precursors are major constituents in highly complex and compositionally variable electrochemical fluorination AFFF formulations, especially legacy electrochemical fluorination (ECF) foams (Backe et al. 2013; Houtz et al. 2013; Place and Field 2012). In contrast, fluorotelomerization foams contain partially fluorinated homologues differing by C_2F_4 units (Backe et al. 2013; Houtz et al. 2013). Long-chain species were mainly used in fluorotelomer-based AFFFs until 2016, when manufacturers switched to short-chain "C_6 foams" (USEPA 2018).

Most environmental compartments affected by AFFF-derived PFASs are found near firefighting training sites or storage facilities. Therefore, many ongoing studies are centered around military bases, petroleum-processing and industries, and airports. The runoff from fire training sites has led to PFAS contaminations up to 10,000 ng L^{-1} in potable water and 34,000 ng L^{-1} in groundwater (Gobelius et al. 2017; Jakobsson et al. 2014). Discharge of PFASs from an airport area to the surrounding river was reported to be approximately 7000 mg day^{-1} (Koch et al. 2019). Additionally, the source tracking of high levels of PFASs in the effluent of various industrial WWTPs is linked to AFFF practice and consequent transport of AFFF-related ingredients to the wastewater (Houtz et al. 2016). Emergency fire quenching techniques are common historic and ongoing practices for vehicle, train, and airplane accidents. For example, in a train accident in 2013 in the town of Lac-Mégantic in Canada, about 33,000 L of concentrated aqueous film-forming foam (AFFF) were applied (Mejia-Avendaño et al. 2017). Two years after this incident, a distinctive level of PFASs across different types of environmental samples was found, in which perfluoroalkyl carboxylic acids were present at higher relative abundance compared to the year of the accident. Explosions in petroleum industries have also been reported. For instance, a fire that occurred at Lester B. Pearson International Airport, Canada, led to the deployment of 45,000 L AFFF (Milley et al. 2018).

Due to the advancement of high-resolution mass spectrometric techniques, PFASs derived from AFFF have been progressively identified. Notable studies that report a large variety of PFAS species include, but are not limited to, the work of D'Agostino and Mabury (2014), Barzen-Hanson et al. (2017), Mejia-Avendaño et al. (2017), and Nickerson et al. (2020). Nickerson and co-workers (2020) found that even at historic AFFF release sites, up to 97% of PFASs may be polyfluorinated

PFAA precursor compounds. However, due to the complexity of AFFF-derived PFASs, numerous questions regarding their speciation at contaminated sites still exist. Furthermore, no standardized, inclusive library of AFFF-derived PFASs exists, and many research groups working on non-targeted PFAS analysis have created their own.

2.2.3 Wastewater Treatment Plants and Biosolids

PFASs have found their way to wastewater treatment systems. However, the transformation processes in conventional biological treatment and advanced oxidation processes (AOPs) in which hydroxyl radicals are utilized may lead to precursor transformation, but are not sufficient to remove all PFAS residuals from the reclaimed water (Nzeribe et al. 2019). PFOS and PFOA are often reported as the primary forms of PFASs in municipal WWTPs (Houtz et al. 2016). Considering the higher solubility of PFOA, it has been found to be a dominant pollutant in sewage sludge at as high as 298 ng g^{-1}_{dw} (Yan et al. 2012). However, PFOS possesses a higher sorption tendency towards the sludge compared to PFOA (Milinovic et al. 2016). In addition, short-chain PFAS ($<C_6$) concentrations seem to be higher in sewage sludge compared to longer-chain compounds (Yan et al. 2012), which suggests transformation of precursors through the WWTP processes.

A significant concentration of untreated PFASs and their associated residuals are expected to reside in recycling fertilizers or biocomposts (Brändli et al. 2007). The presence of PFASs in biosolids is a critical issue because of their annual land application is reported around 7 million tons (55%) in the U.S. (USEPA 2007), and about 4.5 million tons (41%) in the European Union (Gottschall et al. 2017). Studies have reported that land application of PFAS-containing biosolids will result in contamination of the vadose zone that ultimately transfers into groundwater, potable water resources, crops, and dairy products (Gribble et al. 2015; Krepich 2019). Studies in Switzerland have reported up to 250 μg kg^{-1}_{dw} of total PFASs in soil composts (Brändli et al. 2007). In another investigation in Paris, France, the level of PFOS in raw sludge was found to be as high as 1241 μg kg^{-1}_{dw} (Brändli et al. 2007). However, besides PFAAs, polyfluorinated precursor compounds such as sulfonamides, fluorotelomer sulfonates, and polyfluoroalkyl phosphate diesters have been detected in biosolids (Lazcano et al. 2020), indicating incomplete precursor transformation in WWTPs.

2.2.4 Landfill Leachate

Landfills receive a variety of consumer products, such as carpets, textiles, paper, packaging, and often biosolids. Abiotic and biotic processes within the landfill lead to desorption, precursor transformation, and eventually leaching (Hamid et al. 2018). Previous studies have reported PFCAs to be the most abundant species in landfill leachate (20-90% of ∑PFASs), especially shorter-chain C_4-C_7 compounds due to their higher mobility in aqueous environments (Huset et al. 2011; Allred et al. 2014; Yan et al. 2015; Lang et al. 2017). However, a variety of polyfluorinated PFAA precursor classes have been detected, including fluorotelomers, perfluoroalkyl sulfonamide derivatives, and polyfluoroalkyl phosphate esters (PAPs) (Allred et al. 2014; Hamid et al. 2018).

2.2.5 Other Sources

Other PFAS sources that are associated with agricultural practices may include shredded recycled cardboard (SRC), waste paper, and dehydrated paper sludge (DPS) that are widely used for different purposes due to highly moisture-absorbing properties, lightweight, resistant to fungal growth and low density. For example, the total PFOA concentration in SRC, DPS, and recycled wood shaving has been reported by 9, 5, and 4 μg kg^{-1}, respectively (Fernandes et al. 2019). PFOS

has also been reported but at a lower concentration by 1.9 and 3.9 μg kg^{-1} in SRC and DPS, respectively (Fernandes et al. 2019). Also, ash products (i.e., poultry litter) obtained from incineration have been applied as a soil amendment to enhance its quality and nutrients, which are recognized as PFAS contaminating vectors. The ashes collected from the incineration of meat, bonemeal, and poultry litter contained PFOA (0.74-0.89 μg kg^{-1}) and PFOS (0.48-0.60 μg kg^{-1}) (Fernandes et al. 2019). There are several other sources with very limited data which are recognized the sources with minimum risks regarding their geospatial distribution, such as metal fabrication, textile process, furniture and plastic industries (Guelfo et al. 2018).

2.3 Environmental Forensics via FT-ICR MS Analysis

Fourier-transform ion cyclotron resonance mass spectrometry is an emerging analytical approach that offers the highest mass resolution and mass accuracy currently achievable. It can be paired with different selective ionization modes to target specific functional groups, such as electrospray ionization (ESI) or atmospheric pressure photoionization (APPI). The ultrahigh resolving power of FT-ICR MS has advanced the field of "petroleomics", i.e., the characterization of petroleum at the molecular level, and therefore enabled the direct characterization of complex organic sample mixtures without prior fractionation (Lobodin et al. 2013). At a mass range of about 50-1500 Da, it can measure mass-to-charge ratios *m/z* with sub-ppm error.

FT-ICR MS is based on the principles of cyclotron movement, i.e., the circular motion of ions in a strong magnetic field (Marshall et al. 1998). Ionized analytes are introduced into a series of octopoles. The magnetic field causes the ions to resonate at their cyclotron frequency, which is directly related to their *m/z*. After accumulation in the octopoles, the ions are pulsed to the ICR cell where an oscillating electric field is applied. This excitation serves to accelerate ions into a larger orbital radius measured by detector plates on opposite sides of the cell. The detector measures the cyclotron frequency of the ions and uses a Fourier transform to produce a frequency spectrum. The measured frequencies are then converted to a mass spectrum using the relationship between frequency and *m/z*.

The analyses performed via FT-ICR MS as performed here are qualitative in nature for two main reasons: (1) Analyte ionization is selective, i.e., the extent to which analytes of different molecular composition or structure are converted into detectable ions is variable. The same is true for other ESI-coupled mass spectrometers such as QTOF and Orbitrap. Direct quantitation in samples would require commercially available calibration and internal standards for each species of interest. (2) The complex sample mixtures are not chromatographically separated, and their detector response may be impacted by co-occurring target analytes or background matrix ions. In the future, this limitation can be eliminated by coupling liquid chromatography with subsequent FT-ICR MS detection.

The unique ability of FT-ICR MS has led to its use for forensic applications and source tracking of petroleum hydrocarbons. Stanford et. al. (2006) and Teräväinen et. al. (2007) characterized the molecular composition of vacuum gas oil distillation cuts and crude oil distillation fractions and found that different fractions had unique compositional profiles. Corilo et al. (2013) applied principal component analysis (PCA) to differentiate two different sources of spilled weathered oil. Relative abundances of heteroatom classes and double bond equivalent (DBE) distributions were used as input variables for the PCA. Sample clustering in the scores plot traced the detected compounds to distinct sources. The resulting loadings plot highlighted heteroatom classes primarily responsible for the distinction between potential release sources. PCA also enabled the

identification of polar petroleum markers that are highly resistant to biodegradation. Another useful graphical representation of molecular composition is a van Krevelen diagram (VKD) with the O/C ratio of all sample analytes on the x-axis and H/C ratio on the y-axis. The VKD was originally applied to represent bulk elemental compositions in dissolved organic matter (DOM) samples and to trace potential source rocks from oil and gas products (van Krevelen 1950).

FT-ICR MS has advanced the analytical capabilities of many different types of complex mixtures beyond petroleum contamination, such as natural organic matter (NOM), DOM, and biological mixtures of proteins and lipids (He 2009; Jiang 2017). The thousands of elemental compositions assigned by FT-ICR MS enable an unprecedented understanding of sample composition, but they also challenge data interpretation. For non-fluorinated matrices such as petroleum hydrocarbons, the software application PetroOrg® (Corilo 2014) was developed at the National High Magnetic Field Lab (NHMFL). For fluorinated analytes, an automated workflow or software package does not yet exist.

Our preliminary analyses of an AFFF mixture on a custom-built 9.4 Tesla FT-ICR mass spectrometer had initially demonstrated the unique capabilities of this analytical technique. The requirement for ultrahigh resolving power in excess of that achievable by QTOF or Orbitrap MS is highlighted in Figure 3. A mass scale zoom inset at *m/z* 557 shows resolution of two unknown compounds that have the same nominal mass-to-charge ratio (*m/z* 557) but that differ in exact mass by 2.47 mDa, roughly the mass of five electrons. Importantly, these compounds would not be identified by any other mass spectral technique and thus remain undetected.

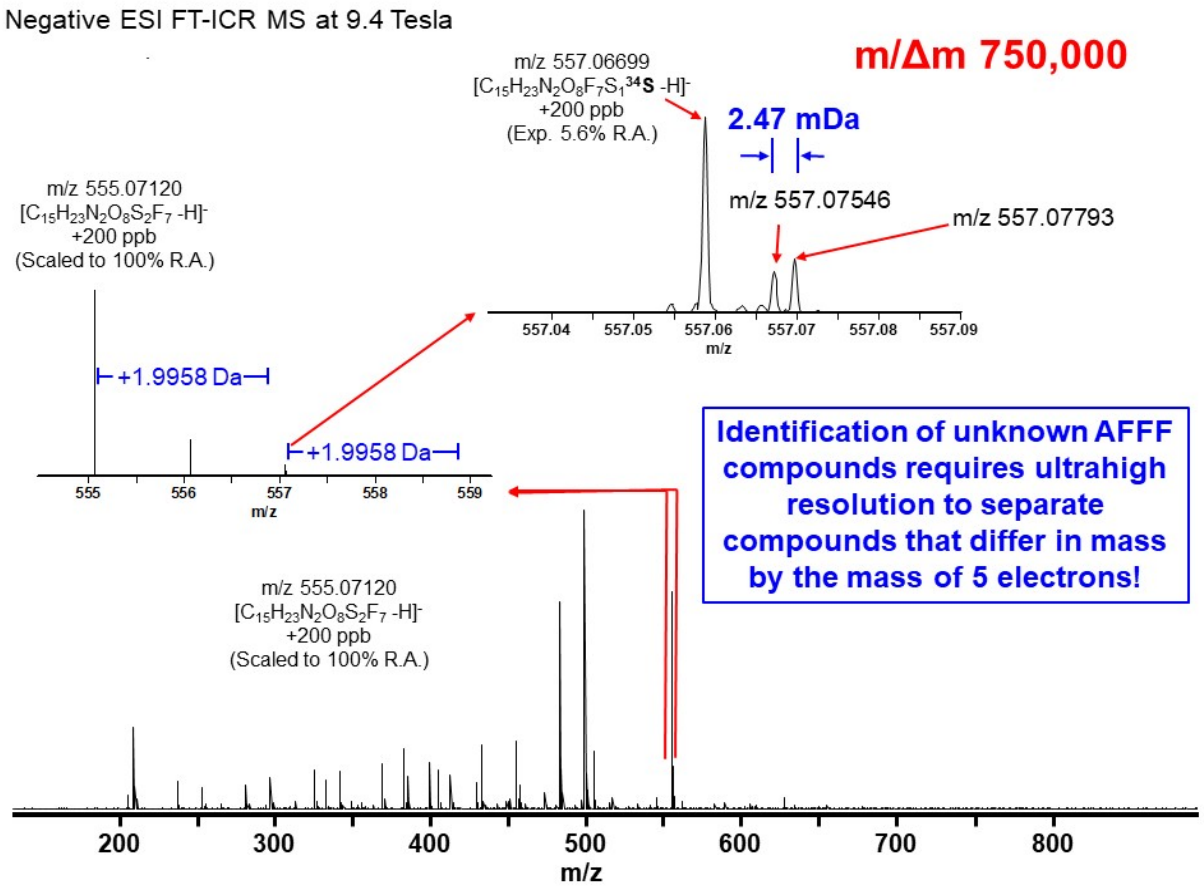

Figure 3: FT-ICR mass spectrum of a 3M electrofluorination AFFF sample with mass scale zoom inset at *m/z* 555-559 (top, left) and *m/z* 557 (top, right). Identification of an unknown, sulfur-containing fluorinated compound is confirmed by the ^{34}S isotopologue at 1.9958 Da higher than the ^{32}S monoisotopic peak that could only be resolved from an unknown compound (top right) at resolving power ($m/\Delta m_{50\%}$) of 750,000 (approximately an order of magnitude higher than qToF, and ~6 times higher than Orbitrap). Resolution of these two isobaric compounds requires theoretical mass resolving power of ~222,000 at *m/z* 557 if the peaks are equal in abundance. Only FT-ICR MS is capable of resolving *m/z* 557.07546 from *m/z* 557.07793, two analytes that differ in mass by roughly the mass of five electrons. Importantly, these compounds would not be resolved on lower resolution systems, and thus would remain undetected.

3 MATERIALS AND METHODS

3.1 Sample Locations and Collection

Site A. Site A is an Air Force Base with historical AFFF application and multiple potential non-DoD sources upgradient and downgradient, some of which potentially unknown. At both on- and off-base groundwater wells, groundwater samples were collected by DoD-approved KOMAN Government Solutions (KGS) and their subcontractor Terracon with a company of the CSU research team. Before sample collection, wells were purged using a Peristaltic Pump (Geotech Environmental Equipment, Inc.) until stabilization of field parameters (Park et al. 2020). The water quality (pH, specific conductivity, temperature, redox potential, and dissolved oxygen) was measured using a Hanna multi-microprocessor. The turbidity was recorded by a Hach turbidimeter (model 2100P). New polyethylene pumping tubes (fluoropolymer-free) were used at all sampling sites (Barzen-Hanson et al. 2017). Decontamination procedures were performed per current applicable guidance and standard operating procedures. The depths of the wells varied from 13 to 32 m. Groundwater samples were collected in new single-use PFAS-free HDPE sample containers with unlined caps. Bottle volumes ranged from 250 mL to 1 L. Sample bottles were filled to 60-70% of their total volume to enable subsequent in-bottle extraction. A travel blank was kept sealed throughout the sampling campaign to minimize potential cross-contamination. Field blanks were exposed to open air at each sampling location for two hours. All bottles were immediately placed in a cooler filled with ice and transferred to Colorado State University for sample extraction.

Site B. Site B is a Naval Air Station with ppm-level aqueous PFASs, where multiple electrochemical fluorination and fluorotelomer AFFFs have been used. A WWTP as well as on-base landfills are potential contributors to the local aquifer contamination with PFASs. The WWTP has historically treated wastewater from the firefighting training area retention fuel/water separator. Groundwater samples and WWTP effluent sample were provided to Colorado State University by the U.S. DoD in HDPE bottles.

Site C. Site C is a Naval Air Station where multiple types of AFFF were used. No other nearby PFAS sources are known or suspected, other than surrounding farm fields and a runoff creek that possibly carries PFASs to the ocean through the base from up the watershed urban/industrial areas. Groundwater samples were provided to Colorado State University by the U.S. DoD in HDPE bottles.

AFFF Sample. The AFFF sample was a 3M electrochemical fluorination product that was generously donated to us by Dr. Paul Hatzinger (APTIM).

3.2 Sample Extraction and Processing

Only fluoropolymer-free equipment, solvents, and supplies were used for sample preparation. Appropriate personal protective equipment, including new nitrile gloves for each sample, were worn during sample preparation and analysis. PFAS standards were purchased from Wellington Laboratories. Only HPLC-grade water and ultra-high purity methanol were used for standard preparation and dilution as numerous organic substances are typically detectable in deionized (DI) water by FT-ICR MS.

Two extraction methods for PFASs in spiked water samples were evaluated: (1) liquid-liquid extraction (LLE) based on Allred et al. (2014) and (2) sequential extraction by a weak anion exchange (WAX) solid-phase extraction (SPE) cartridge followed by a weak cation exchange

(WCX) SPE cartridge based on D'Agostino & Mabury (2014). Using a mix of 24 PFASs (Wellington Laboratories Cat. No. PFAC-24PAR) as well as the AFFF sample, the highest recoveries were found for LLE using ethyl acetate with 10% trifluoroethanol with ≥80% for C_4-C_{14} PFASs in the commercial mixture via liquid chromatography coupled with a triple quadrupole mass spectrometer in negative ionization mode (LC/ESI$^-$/QQQ-MS) and ≥75% for PFASs in dilute AFFF (via liquid chromatography coupled with a quadrupole time-of-flight mass spectrometer in both negative and positive ionization modes, LC/ESI/QTOF-MS), with the exception of non-fluorinated polyethoxylate surfactants (recovery < 10 %) in positive ionization mode. In contrast, recoveries for higher-molecular weight PFASs using sequential SPE were poor (Table A 1 in Appendix A). Consequently, LLE was chosen for sample extraction prior to FT-ICR MS analysis. In future work, matrix spike samples should be included at the frequency of one per batch of samples extracted for each media type (i.e., groundwater, wastewater, AFFF, other media) to ensure that the techniques used for both extraction and analysis can handle the matrix interferences present in each sample media type.

Field sample bottles were first weighed against empty bottles to determine the water volume collected in the field. Subsequently, an aliquot of ethyl acetate (HPLC-grade, 99.9 %) with 10 % trifluoroethanol (99.8 % Extra Pure) at 25 % of the water volume was added. The mixture was shaken manually for one minute, ensuring contact of the separate organic phase with all bottle walls, and subsequently on an orbital shaker for an additional 30 minutes. The organic phase was then recovered, its volume recorded, and the same volume of fresh organic solvent was added to repeat the extraction step. A total of three extraction steps per bottle were performed. The recovered organic solvent was captured in new, pre-baked 60-mL VOA vials, and the extracts were blown to dryness using ultrahigh-purity nitrogen gas. Note that commonly used polypropylene Falcon centrifuge tubes were not used in this step as the testing of extraction blanks showed leaching of organic chemicals from these containers.

Blank samples were processed and analyzed via LC/ESI$^-$/QQQ-MS to verify the absence of cross-contamination. One blank sample per day of laboratory extraction was collected from PFAS-free HPLC-grade water in HDPE containers. Blanks underwent the same sample processing as the field water samples, starting with LLE.

The dry VOA vials were covered with parafilm, screw-capped, and sent to the National High Magnetic Field Laboratory for analysis.

3.3 Sample Analysis and Spectrum Processing

Dry sample extracts were diluted 4:1, and AFFF diluted 1:1000 in ultrahigh-purity methanol prior to analysis by negative ion electrospray ionization. Sample solution was infused via a microelectrospray source (Emmett et al. 1998) (50 µm i.d. fused silica emitter) at 500 nL/min by a syringe pump. Typical conditions for negative ion formation were: emitter voltage, -2.9-3.0 kV; S-lens RF level 45%; and heated metal capillary temperature, 350 °C.

Sample extracts were analyzed with a custom-built hybrid linear ion trap FT-ICR mass spectrometer equipped with a 21 T superconducting solenoid magnet (Hendrickson et al. 2015, Smith et al. 2018). Ions were initially accumulated in an external multipole ion guide (1-5 ms) and released *m/z*-dependently by decrease of an auxiliary radio frequency potential between the multipole rods and the end-cap electrode (Kaiser et al. 2013). Ions were excited to *m/z*-dependent radius to maximize the dynamic range and number of observed mass spectral peaks (32-64%)

(Kaiser et al. 2013), and excitation and detection were performed on the same pair of electrodes (Che et al. 2014). The dynamically harmonized ICR cell in the 21 T FT-ICR is operated with 6 V trapping potential (Kaiser et al. 2013; Boldin & Nikolaev 2011). Time-domain transients of 3.1 seconds were acquired with the Predator data station that handled excitation and detection only, initiated by a TTL trigger from the commercial Thermo data station, with 100 time-domain acquisitions averaged for all experiments (Blakney et al. 2011). Mass spectra were phase-corrected (Xian et al. 2010) and internally calibrated with 10-15 highly abundant homologous series that span the entire molecular weight distribution based on the "walking" calibration method (Savory et al. 2011). Experimentally measured masses were converted from the International Union of Pure and Applied Chemistry (IUPAC) mass scale to the Kendrick mass scale (Kendrick 1963; McLafferty & Turecek 1993; Hughey et al. 2001). Peaks with signal magnitude greater than 6 times the baseline root-mean-square (rms) noise at *m/z* 500 were exported to the peak lists (Corilo 2014).

4 RESULTS AND DISCUSSION

The following section presents the development of our spectral processing for PFAS identification, a forensic analysis for the collected spectra, and measures for quality assurance (QA) and quality control (QC). The PFAS species identified in this study are classified as either "knowns" or "unknowns". "Known" PFASs are those molecular formulas with an exact match in one of the two databases used. The first database is the PFAS database compiled by the Organisation for Economic Co-operation and Development that contains 4730 species (OECD 2021). The second database is a list of 2154 species generously provided to us by Dr. Christopher Higgins at the Colorado School of Mines. "Unknown" PFASs are molecular formulas that had no exact matches in either of the two databases.

4.1 Total Peak Detections via Negative-Ion FT-ICR MS

Table 1 shows the number of peaks detected (i.e., signal-to-noise > 6) in the analyzed samples. With the exception of the AFFF sample, more than 10,000 peaks were detected in all of the samples. The contribution from dissolved organic matter (DOM) varied greatly, from only 114 peaks in the AFFF sample to 7757 peaks in the WWTP effluent sample.

Table 1: Numbers of (1) total peaks detected, (2) peaks identified as DOM, (3) peaks identified as known PFASs, (4) peaks identified as unknown PFASs, (5) isotopologues, and (6) remaining unassigned peaks.

Location	Sample ID	Total Peaks	DOM Peaks	Known PFASs	Unknown PFASs	Isotopes	Unassigned Peaks
N/A	AFFF	9,247	114	193	96	166	8,678
Site A	ONBASE 1	14,990	3,364	141	106	118	11,261
	ONBASE 2	20,718	5,625	124	37	70	14,862
	OFFBASE 1	14,012	1,753	72	13	39	12,135
	OFFBASE 2	19,019	5,993	142	51	80	12,753
	OFFBASE 3	18,637	5,650	130	51	66	12,740
	OFFBASE 4	18,144	5,686	72	5	29	12,352
SITE B	SITE B 1	15,624	1,083	130	48	91	14,272
	WWTP	14,892	7,757	63	42	42	6,988
SITE C	SITE C 1	15,361	1,807	76	13	38	13,427
	SITE C 2	12,747	3,856	159	34	97	8,601

4.2 Identification of Dissolved Organic Matter Species

All spectra were initially processed with PetroOrg® for the identification of DOM species. Prior to PFAS molecular formula assignment, DOM species were removed from the peak lists to avoid false assignments and increase spectral processing efficiency. Select examples of DOM speciation are highlighted below to illustrate the highly variable composition between AFFF, groundwater, and wastewater.

The AFFF sample had by far the lowest number of DOM peaks with 114 assigned formulas. Most of these species were aliphatic in nature with an H/C ratio above 1.5 (Figure 4). The heteroatom class distribution revealed high relative abundances by sulfur-containing O_xS_1 species, dominated by the O_4S_1 species $C_8H_{18}O_4S$. This species was identified as octyl sulfate. Alkyl sulfates are non-fluorinated hydrocarbon surfactants that have been used as ingredients in certain (though not all)

AFFF formulations such as 3M (after 1988), Buckeye, Chemguard, and National Foam (Garcia et al. 2019). It is thus likely that the species identified via PetroOrg® as DOM based on CH_2 series were non-fluorinated hydrocarbon surfactants.

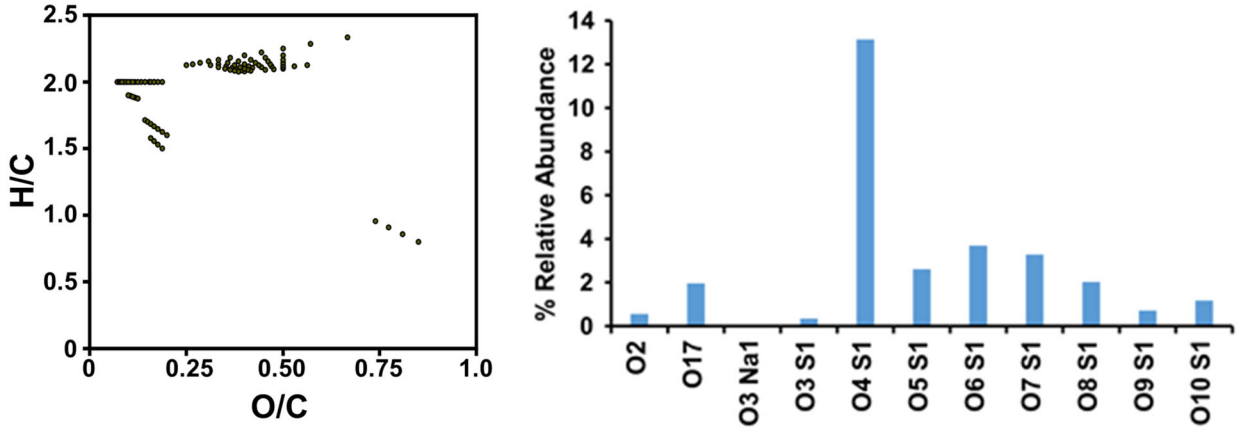

Figure 4: Van Krevelen diagram (left) and heteroatom class distribution for DOM species detected in the AFFF sample.

The groundwater sample from Site B 1 had 1083 assignments for DOM species that included unsaturated species with a lower H/C ratio than the AFFF sample (Figure 5). O_2 species were the most abundant heteroatom class. However, various O_xS_1 classes were detected, again with O_4S_1 dominating. These results indicate that hydrocarbon surfactants many still be present in this groundwater sample.

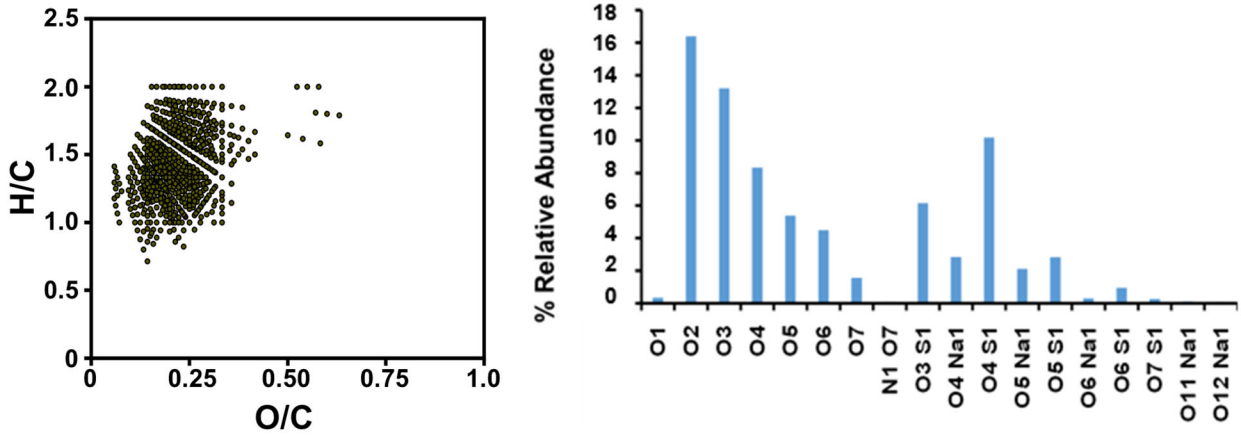

Figure 5: Van Krevelen diagram (left) and heteroatom class distribution for DOM species detected in the Site B 1 sample.

The WWTP effluent sample from Site B revealed DOM species with a higher degree of oxygenation (i.e., O/C ratio), possibly due to aerobic biotransformation processes within the WWTP (Figure 6). The heteroatom class distribution was dominated by O_x rather than sulfur-containing classes. In comparison to the results from the AFFF-impacted groundwater, these

findings indicate that hydrocarbon surfactants may likewise be used for forensic source tracking purposes.

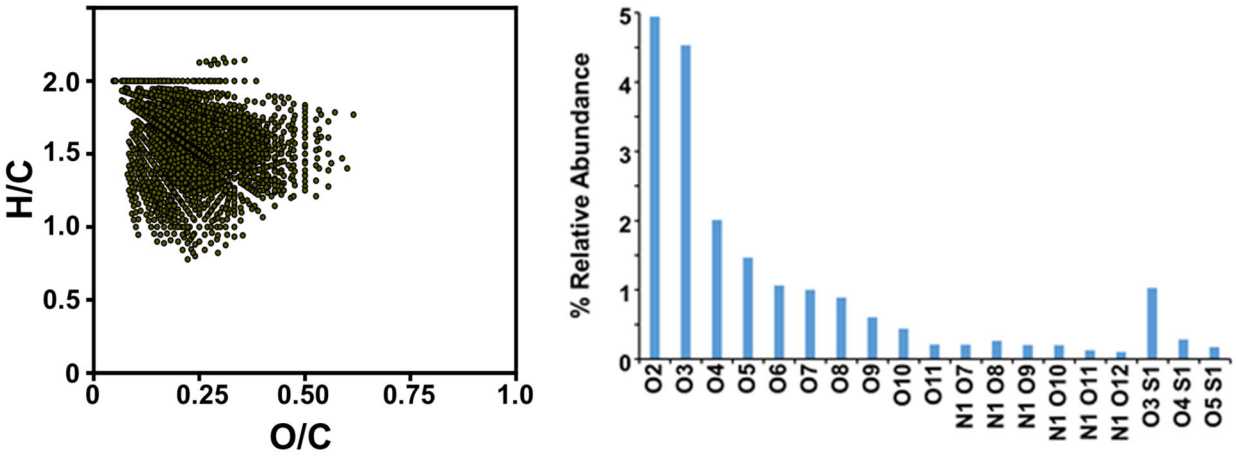

Figure 6: Van Krevelen diagram (left) and heteroatom class distribution for DOM species detected in the WWTP sample.

4.3 Analysis of Existing PFAS Databases and Rule Development

To develop a set of rules that can aid in molecular formula assignment during non-targeted spectral processing (see below), we initially analyzed the two PFAS databases as well as a Suwannee River DOM sample (Figure 7). The histograms for the frequencies of mass defects (Δm = exact mass – nominal mass) revealed that almost all DOM species possess a positive mass defect, while PFASs are almost evenly split into species with positive and negative mass defect. Consequently, the level of confidence for PFAS molecular formula assignments to analytes with negative mass defects is higher than to those with a positive mass defect.

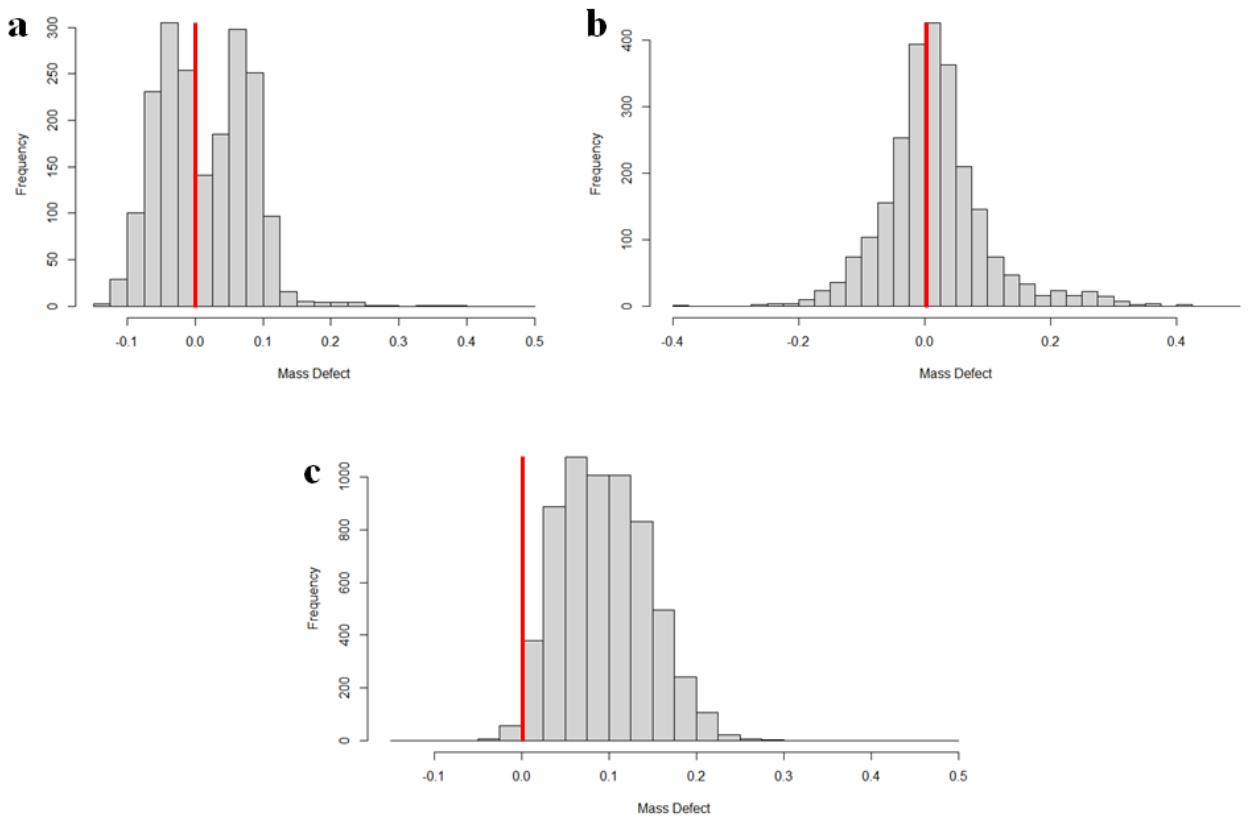

Figure 7: Histograms showing the frequency of mass defects for a) PFASs in the Colorado School of Mines database, b) PFASs in the OECD database, and c) Suwannee River DOM. The red line indicates the border between negative and positive mass defects.

Furthermore, statistical analyses of element counts (Figure 8) and double bond equivalents (DBEs, not shown here) in known PFASs were conducted to establish element number and ratio restrictions that will further aid in narrowing down the number of potential formula assignments and increase the confidence in correct identifications. Based on these analyses, the following rules were established for non-targeted analysis:

$3 < F$
$S \leq 3$
$P = 0$
$P = 1$ only if $O \geq 3$
$N < 3$
$O + S + N \geq 1$

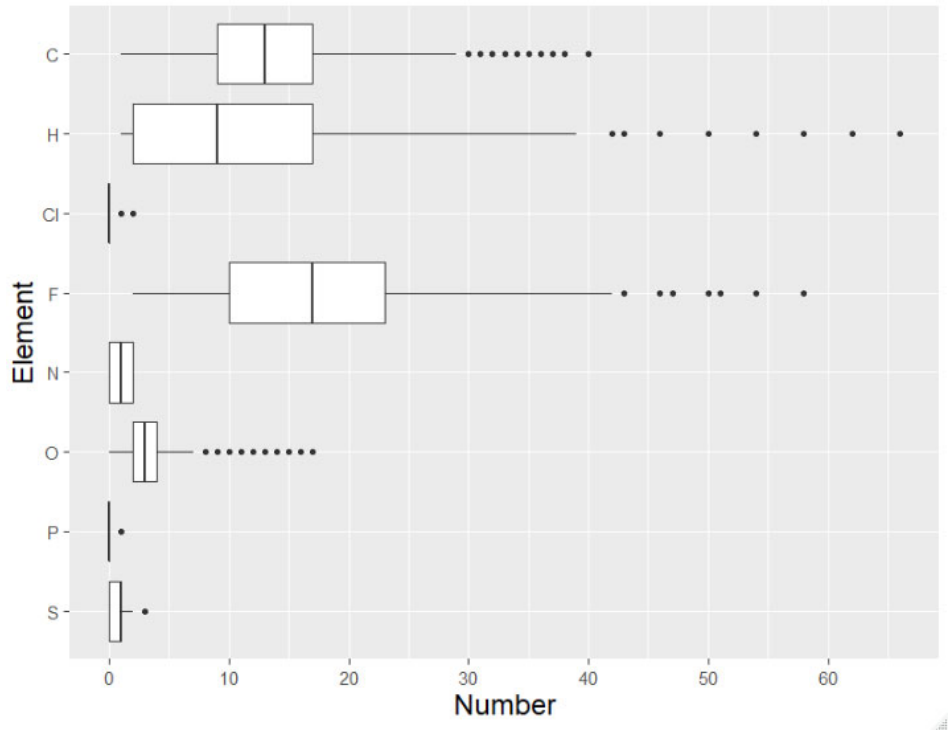

Figure 8: Element counts for PFASs in the Colorado School of Mines database. The central bold line is the median, and the box is the interquartile range. The horizontal lines extend to the smallest and largest values that are no greater than 1.5x the interquartile range. The dots represent outliers beyond this range.

4.4 Code and Workflow Development for FT-ICR Mass Spectrum Processing

After rule development, a spectral processing workflow was developed and applied to all samples for PFAS identification (Figure 9). As a first step, a suspect screening for known PFASs listed in the two databases was conducted in the Jupyter Lab environment (V.4.4.0), applying a custom-written script in Python. Matches of computed neutral masses were limited to a ppm error <0.2 and validated by presence and correct abundance of ^{34}S and ^{37}Cl isotopes, if applicable. After isotope validation, all isotopologues including ^{13}C were eliminated from the peak list for further processing to ensure that only one isotopologue per PFAS species would be reported at the end. PFASs identified as knowns during suspect screening were assigned a Confidence **Level 1** in the style of high resolution mass spectrometry confidence levels suggested by Schymanski and co-workers (2014).

For the remaining peaks not identified as PFASs during suspect screening, a non-targeted analysis was conducted. First, a theoretical PFAS library was developed in which exact masses for a variety of element and isotope compositions was calculated for matching with detected *m/z* values. The library was integrated into the adopted UltraMassExplorer (UME, Leefmann et al. 2019) software (V.2.2.0) in the R programming environment (V.1.2.5033) using the Shiny package. Due to the large size of the library, UME was executed on High Performance Computing clusters maintained by the Engineering Technology Services at Colorado State University.

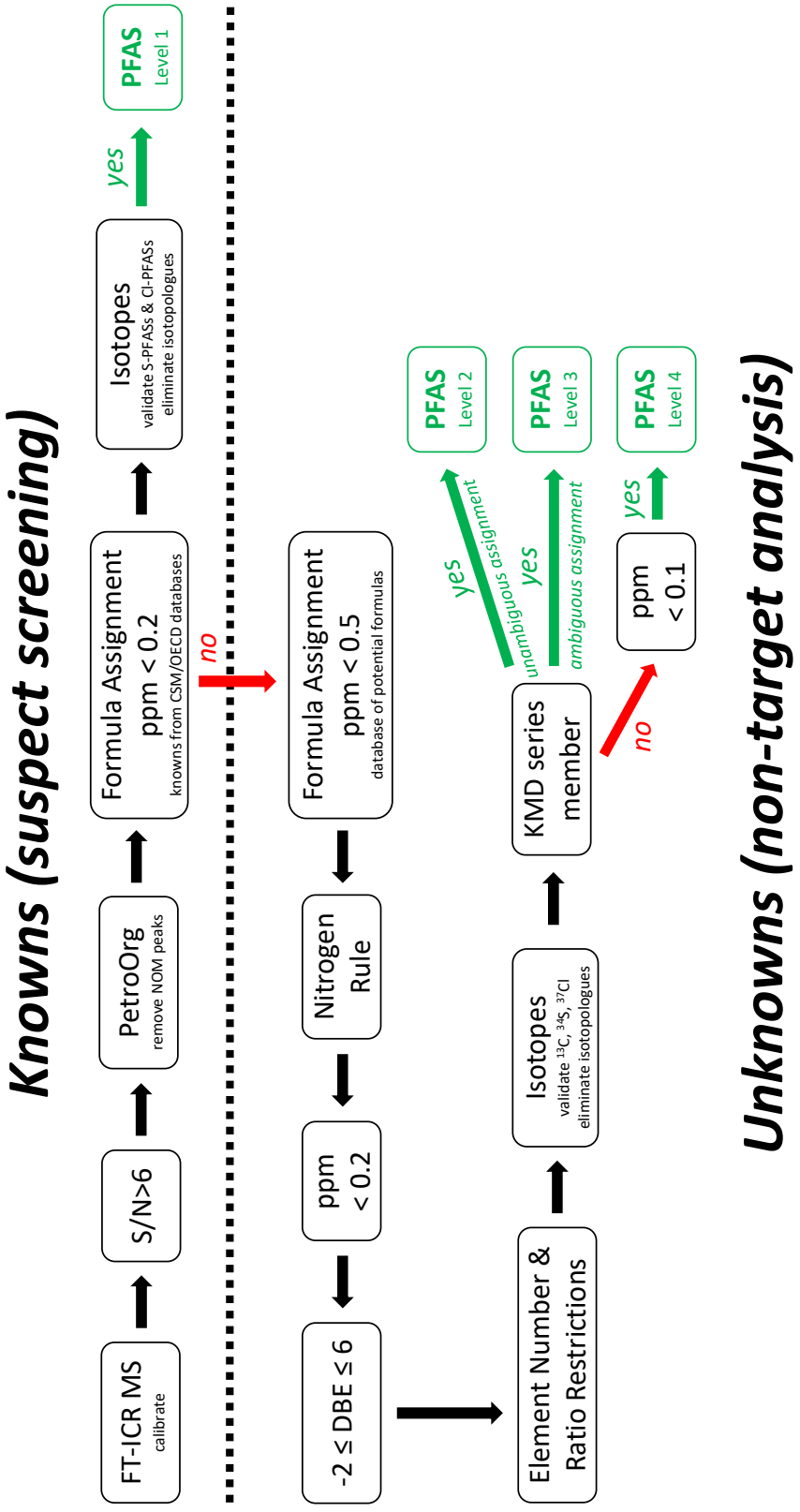

Figure 9: Workflow for molecular formula assignment to PFASs detected via FT-ICR MS. For details please see the text.

Subsequently, several steps were taken to further restrict the number of assigned formulas in order to assign one unique formula with the highest possible level of confidence. After applying the nitrogen rule (Tureček & McLafferty 1993), the ppm error was restricted to <0.2, DBEs were limited to ≥-2 and ≤6, and the element number and ratio restrictions determined in the previous step were applied. Isotope presence and abundances were validated where applicable, and ^{34}S, ^{37}Cl and ^{13}C isotopologues were again eliminated from the list after validation. Then, members of CF_2 Kendrick mass defect (KMD) series, which had to include at least one member with an unambiguous assigned molecular formula, were identified to verify consistent assignments within each series (Hughey et al. 2001; Garcia et al. 2019). CF_2 KMD series members with an unambiguous assigned molecular formula were identified as **Level 2** PFAS. Members of CF_2 KMD series with ambiguous molecular formulas were assigned an unambiguous formula from matching with their identified CF_2 KMD series and classified as **Level 3** PFAS. For unknown species which were not a member of a CF_2 KMD series, a more stringent ppm error range of <0.1 was applied. After this final step, species with one unambiguous assignment were classified as **Level 4** PFAS, while species with ambiguous assignments were left unidentified.

4.5 Identification of PFASs

Due to the extensive amount of data collected, we will focus our discussion of PFAS identification on the three samples highlighted above, namely the AFFF sample as well as the groundwater and WWTP effluent samples from Site B. Their original FT-ICR mass spectra are shown in Appendix A for reference. Furthermore, our analysis will only include known and unknown PFASs identified at Confidence Levels 1 and 2. No specific PFASs (only CF_2 series with ambiguous formula assignments) were identified in these samples at Confidence Level 3. At the lowest Level 4, thousands of unambiguous formulas were assigned, however, at the lowest confidence and likely not needed for forensic analysis. However, all peaks with unambiguous assigned formulas from all samples are included in the mass spectral library submitted along with this report (see below).

In the AFFF sample, 193 known PFASs were detected, while 130 and 63 known PFASs were identified in the groundwater and WWTP effluent samples, respectively (Table 1). In addition, various new PFASs were detected. In the AFFF sample, 96 novel PFASs were identified. Table 2 lists novel species and classes that were identified in the AFFF sample at the highest confidence level for unknowns (Level 2) as part of a CF_2 KMD series. While structural information cannot be provided from FT-ICR MS analysis – and is not necessarily required for forensic analysis – general molecular formulas for the classes are shown. Besides C, H, and F, the 22 novel classes in the ECF AFFF contain varying numbers of chlorine, nitrogen, oxygen, sulfur, and phosphorus. The same is true for the 13 novel classes (and 48 novel PFAS species in total) identified in the groundwater sample (Table 3). However, these two samples had only two novel classes in common ($C_nH_7ClF_{2(n-4)+1}O_7P$ and $C_nH_7Cl_2F_{2(n-7)+1}N_2O_9$). Note that this analyzed AFFF sample stemmed from a different source and was likely never used at Site B.

In contrast, the 11 novel PFAS classes detected in the WWTP effluent sample from Site B (Table 4) exclusively belonged to NO_x classes, i.e., they had one nitrogen and neither sulfur nor phosphorus. Only one of the classes contained a chlorine atom. A total of 42 novel PFAS species were detected in WWTP the effluent sample.

Table 2: Novel PFAS classes discovered in the ECF AFFF sample including detected series homologues and their molecular formulas, theoretical and experimental masses, ppm error, and CF_2 Kendrick mass defect (KMD).

Molecular Formula	Theor. Mass	Exp. Mass	ppm Error	CF_2 KMD	Class Molecular Formula
C26H38F6N2O3S3	636.19488	636.19496	0.127	-0.2355	$C_nH_{38}F_{2(n-23)}N_2O_3S_3$
C27H38F8N2O3S3	686.19168	686.19176	0.109	-0.2355	
C25H38F4N2O3S3	586.19807	586.19806	-0.022	-0.2355	
C27H35Cl2F8NO2S	659.16378	659.16373	-0.083	-0.2059	$C_nH_{35}Cl_2F_{2(n-23)}NO_2S$
C26H35Cl2F6NO2S	609.16697	609.16698	0.003	-0.2059	
C25H35Cl2F4NO2S	559.17017	559.17020	0.050	-0.2059	
C25H34F8N2O3S3	658.16038	658.16035	-0.054	-0.2024	$C_nH_{34}F_{2(n-21)}N_2O_3S_3$
C24H34F6N2O3S3	608.16358	608.16363	0.084	-0.2024	
C23H34F4N2O3S3	558.16677	558.16681	0.067	-0.2024	
C22H33Cl2F12NO5	689.15442	689.15443	0.014	-0.1984	$C_nH_{33}Cl_2F_{2(n-16)}NO_5$
C21H33Cl2F10NO5	639.15761	639.15763	0.025	-0.1984	
C20H33Cl2F8NO5	589.16080	589.16076	-0.081	-0.1984	
C24H32F8N2O4S3	660.13965	660.13965	0.000	-0.1818	$C_nH_{32}F_{2(n-20)}N_2O_4S_3$
C23H32F6N2O4S3	610.14284	610.14290	0.093	-0.1818	
C22H32F4N2O4S3	560.14603	560.14609	0.094	-0.1818	
C24H29F11N2OS3	666.12664	666.12670	0.090	-0.1692	$C_nH_{29}F_{2(n-14)+1}N_2OS_3$
C23H29F9N2OS3	616.12983	616.12988	0.075	-0.1692	
C22H29F7N2OS3	566.13302	566.13308	0.092	-0.1692	
C21H29F5N2OS3	516.13622	516.13632	0.191	-0.1692	
C15H23ClF7N2O8P	558.07688	558.07684	-0.074	-0.1125	$C_nH_{23}ClF_{2(n-12)+1}N_2O_8P$
C14H23ClF5N2O8P	508.08007	508.08005	-0.049	-0.1125	
C13H23ClF3N2O8P	458.08326	458.08325	-0.040	-0.1125	
C17H23ClF11N2O8P	658.07049	658.07040	-0.143	-0.1125	
C16H23ClF9N2O8P	608.07368	608.07368	-0.012	-0.1125	
C20H23F8NO2S3	557.07632	557.07639	0.123	-0.1119	$C_nH_{23}F_{2(n-16)}NO_2S_3$
C18H23F4NO2S3	457.08271	457.08277	0.134	-0.1119	
C19H23F6NO2S3	507.07951	507.07961	0.188	-0.1119	
C18H16ClF13N2O	558.07436	558.07438	0.035	-0.11	$C_nH_{16}ClF_{2(n-12)+1}N_2O$
C17H16ClF11N2O	508.07755	508.07759	0.071	-0.11	
C16H16ClF9N2O	458.08074	458.08079	0.092	-0.11	
C15H16ClF7N2O	408.08394	408.08397	0.070	-0.11	
C19H16ClF15N2O	608.07116	608.07127	0.170	-0.11	
C14H17F13N2O5S	572.06506	572.06496	-0.179	-0.1016	$C_nH_{17}F_{2(n-8)+1}N_2O_5S$
C13H17F11N2O5S	522.06825	522.06826	0.007	-0.1016	
C12H17F9N2O5S	472.07145	472.07144	-0.021	-0.1016	
C11H17F7N2O5S	422.07464	422.07466	0.039	-0.1016	
C15H17F15N2O5S	622.06187	622.06181	-0.095	-0.1016	
C16H17F17N2O5S	672.05867	672.05867	-0.008	-0.1016	
C16H16F18O4S	646.04819	646.04820	0.014	-0.0895	$C_nH_{16}F_{2(n-7)}O_4S$
C14H16F14O4S	546.05457	546.05454	-0.070	-0.0895	
C13H16F12O4S	496.05777	496.05781	0.077	-0.0895	
C15H16F16O4S	596.05138	596.05136	-0.041	-0.0895	
C12H16F10O4S	446.06096	446.06102	0.123	-0.0895	
C10H16F6O4S	346.06735	346.06740	0.137	-0.0895	

Table 2 (continued).

Molecular Formula	Theor. Mass	Exp. Mass	ppm Error	CF_2 KMD	Class Molecular Formula
C13H14F16N2O2S	566.05205	566.05203	-0.041	-0.0882	$C_nH_{14}F_{2(n-5)}N_2O_2S$
C11H14F12N2O2S	466.05844	466.05845	0.021	-0.0882	
C10H14F10N2O2S	416.06163	416.06164	0.014	-0.0882	
C9H14F8N2O2S	366.06482	366.06483	0.006	-0.0882	
C14H14F18N2O2S	616.04886	616.04884	-0.031	-0.0882	
C7H14F4N2O2S	266.07121	266.07122	0.019	-0.0882	
C12H19ClF7N2O6P	486.05575	486.05573	-0.045	-0.0868	$C_nH_{19}ClF_{2(n-9)+1}N_2O_6P$
C11H19ClF5N2O6P	436.05894	436.05887	-0.173	-0.0868	
C10H19ClF3N2O6P	386.06214	386.06213	-0.024	-0.0868	
C14H19ClF11N2O6P	586.04936	586.04930	-0.110	-0.0868	
C13H19ClF9N2O6P	536.05255	536.05254	-0.034	-0.0868	
C14H15Cl2F10N3	485.04833	485.04842	0.169	-0.0793	$C_nH_{15}Cl_2F_{2(n-9)}N_3$
C13H15Cl2F8N3	435.05153	435.05154	0.019	-0.0793	
C12H15Cl2F6N3	385.05472	385.05480	0.194	-0.0793	
C11H15Cl2F4N3	335.05792	335.05798	0.182	-0.0793	
C15H15Cl2F12N3	535.04514	535.04519	0.085	-0.0793	
C16H15Cl2F14N3	585.04195	585.04194	-0.018	-0.0793	
C11H17F8N3O5S2	487.04819	487.04817	-0.045	-0.0793	$C_nH_{17}F_{2(n-7)}N_3O_5S_2$
C10H17F6N3O5S2	437.05138	437.05132	-0.150	-0.0793	
C9H17F4N3O5S2	387.05458	387.05457	-0.024	-0.0793	
C13H17F12N3O5S2	587.04180	587.04175	-0.093	-0.0793	
C12H17F10N3O5S2	537.04499	537.04495	-0.090	-0.0793	
C15H9F14NO	485.04606	485.04606	-0.004	-0.077	$C_nH_9F_{2(n-8)}NO$
C13H9F10NO	385.05245	385.05245	0.002	-0.077	
C14H9F12NO	435.04925	435.04918	-0.174	-0.077	
C12H9F8NO	335.05564	335.05563	-0.038	-0.077	
C17H9F18NO	585.03967	585.03964	-0.059	-0.077	
C16H9F16NO	535.04286	535.04284	-0.053	-0.077	
C11H13F11N2O3S	462.04712	462.04714	0.029	-0.0766	$C_nH_{13}F_{2(n-6)+1}N_2O_3S$
C10H13F9N2O3S	412.05032	412.05032	-0.001	-0.0766	
C12H13F13N2O3S	512.04393	512.04394	0.013	-0.0766	
C13H13F15N2O3S	562.04074	562.04066	-0.142	-0.0766	
C9H13F7N2O3S	362.05351	362.05353	0.044	-0.0766	
C13H19Cl2F7NO3P	471.03678	471.03671	-0.163	-0.0669	$C_nH_{19}Cl_2F_{2(n-8)+1}NO_3P$
C12H19Cl2F5NO3P	421.03998	421.03997	-0.024	-0.0669	
C11H19Cl2F3NO3P	371.04317	371.04310	-0.200	-0.0669	
C10H11F13N2O2S	470.03336	470.03337	0.003	-0.0634	$C_nH_{11}F_{2(n-4)+1}N_2O_2S$
C8H11F9N2O2S	370.03975	370.03975	-0.016	-0.0634	
C9H11F11N2O2S	420.03656	420.03659	0.066	-0.0634	
C7H11F7N2O2S	320.04295	320.04295	0.002	-0.0634	
C12H11F17N2O2S	570.02698	570.02691	-0.125	-0.0634	
C11H11F15N2O2S	520.03017	520.03023	0.106	-0.0634	
C9H7ClF11O7P	501.94423	501.94421	-0.041	0.0237	$C_nH_7ClF_{2(n-4)+1}O_7P$
C7H7ClF7O7P	401.95061	401.95059	-0.070	0.0237	
C8H7ClF9O7P	451.94742	451.94744	0.035	0.0237	
C10H7Cl2F7N2O9	501.94168	501.94174	0.108	0.0263	$C_nH_7Cl_2F_{2(n-7)+1}N_2O_9$
C8H7Cl2F3N2O9	401.94807	401.94813	0.142	0.0263	
C9H7Cl2F5N2O9	451.94488	451.94494	0.134	0.0263	
C11H3Cl2F14NO	500.93681	500.93689	0.146	0.0312	$C_nH_3Cl_2F_{2(n-4)}NO$
C9H3Cl2F10NO	400.94320	400.94327	0.164	0.0312	
C10H3Cl2F12NO	450.94001	450.94008	0.154	0.0312	
C7H3Cl2F6NO	300.94959	300.94965	0.195	0.0312	

Table 3: Novel PFAS classes discovered in the Site B 1 groundwater sample including detected series homologues and their molecular formulas, theoretical and experimental masses, ppm error, and CF_2 Kendrick mass defect (KMD).

Molecular Formula	Theor. Mass	Exp. Mass	ppm Error	CF_2 KMD	Class Molecular Formula
C14H19Cl2F7NO4P	499.03170	499.03166	-0.083	-0.0636	$C_nH_{19}Cl_2F_{2(n-11)+1}NO_4P$
C13H19Cl2F5NO4P	449.03489	449.03483	-0.145	-0.0636	
C12H19Cl2F3NO4P	399.03808	399.03803	-0.147	-0.0636	
C11H11F13N2O3S	498.02828	498.02834	0.115	-0.0601	$C_nH_{11}F_{2(n-5)+1}N_2O_3S$
C10H11F11N2O3S	448.03147	448.03147	-0.015	-0.0601	
C9H11F9N2O3S	398.03467	398.03466	-0.026	-0.0601	
C8H11F7N2O3S	348.03786	348.03787	0.017	-0.0601	
C10H12F8O10	444.03027	444.03025	-0.057	-0.0586	$C_nH_{12}F_{2(n-6)}O_{10}$
C11H12F10O10	494.02708	494.02714	0.118	-0.0586	
C9H12F6O10	394.03347	394.03349	0.053	-0.0586	
C8H6F13NO3S	442.98608	442.98608	-0.009	-0.0144	$C_nH_6F_{2n-3}NO_3S$
C6H6F9NO3S	342.99247	342.99247	-0.004	-0.0144	
C7H6F11NO3S	392.98927	392.98929	0.032	-0.0144	
C5H6F7NO3S	292.99566	292.99566	-0.017	-0.0144	
C9H6F15NO3S	492.98289	492.98297	0.162	-0.0144	
C7H2F13NO3S	426.95478	426.95477	-0.032	0.0179	$C_nH_2F_{2n-1}NO_3S$
C8H2F15NO3S	476.95159	476.95156	-0.063	0.0179	
C6H2F11NO3S	376.95797	376.95796	-0.046	0.0179	
C5H2F9NO3S	326.96117	326.96117	-0.004	0.0179	
C4H2F7NO3S	276.96436	276.96435	-0.053	0.0179	
C9H7ClF11O7P	501.94423	501.94415	-0.161	0.0237	$C_nH_7ClF_{2(n-4)+1}O_7P$
C7H7ClF7O7P	401.95061	401.95061	-0.020	0.0237	
C8H7ClF9O7P	451.94742	451.94740	-0.054	0.0237	
C6H7ClF5O7P	351.95381	351.95380	-0.033	0.0237	
C10H7Cl2F7N2O9	501.94168	501.94171	0.048	0.0263	$C_nH_7Cl_2F_{2(n-7)+1}N_2O_9$
C8H7Cl2F3N2O9	401.94807	401.94815	0.191	0.0263	
C9H7Cl2F5N2O9	451.94488	451.94493	0.112	0.0263	
C12H5F11O5S2	501.94028	501.94023	-0.098	0.0277	$C_nH_5F_{2(n-7)+1}O_5S_2$
C10H5F7O5S2	401.94666	401.94663	-0.090	0.0277	
C11H5F9O5S2	451.94347	451.94348	0.016	0.0277	
C14H6Cl2F12S	503.93756	503.93755	-0.036	0.0302	$C_nH_6Cl_2F_{2(n-8)}S_2$
C12H6Cl2F8S	403.94395	403.94393	-0.063	0.0302	
C13H6Cl2F10S	453.94076	453.94071	-0.115	0.0302	
C8H5F12NO6S2	502.93667	502.93664	-0.061	0.0312	$C_nH_5F_{2(n-2)}NO_6S_2$
C6H5F8NO6S2	402.94305	402.94305	-0.020	0.0312	
C7H5F10NO6S2	452.93986	452.93984	-0.054	0.0312	
C5H5F6NO6S2	352.94625	352.94623	-0.062	0.0312	
C8H4ClF12O5P	473.92933	473.92939	0.128	0.0404	$C_nH_4ClF_{2(n-2)}O_5P$
C7H4ClF10O5P	423.93252	423.93256	0.087	0.0404	
C6H4ClF8O5P	373.93571	373.93579	0.196	0.0404	
C7H6ClF10O3PS2	457.90248	457.90247	-0.036	0.0683	$C_nH_6ClF_{2(n-2)}O_3PS_2$
C8H6ClF12O3PS2	507.89929	507.89930	0.015	0.0683	
C6H6ClF8O3PS2	407.90568	407.90569	0.025	0.0683	
C5H6ClF6O3PS2	357.90887	357.90891	0.102	0.0683	
C4H6ClF4O3PS2	307.91206	307.91201	-0.187	0.0683	
C6H4ClF10O6PS	459.89951	459.89954	0.068	0.0711	$C_nH_4ClF_{2n-2}O_6PS$
C7H4ClF12O6PS	509.89631	509.89632	0.009	0.0711	
C5H4ClF8O6PS	409.90270	409.90274	0.092	0.0711	

Table 4: Novel PFAS classes discovered in the Site B WWTP effluent sample including detected series homologues and their molecular formulas, theoretical and experimental masses, ppm error, and CF_2 Kendrick mass defect (KMD).

Molecular Formul	Theor. Mass	Exp. Mass	ppm Error	CF_2 KMD	Class Molecular Formula
C26H45F6NO4	549.32528	549.32527	-0.021	-0.3604	$C_nH_{45}F_{2(n-23)}NO_4$
C29H45F12NO4	699.31570	699.31568	-0.029	-0.3604	
C27H45F8NO4	599.32208	599.32217	0.137	-0.3604	
C25H45F4NO4	499.32847	499.32849	0.030	-0.3604	
C25H43F6NO4	535.30963	535.30965	0.035	-0.3438	$C_nH_{43}F_{2(n-22)}NO_4$
C26H43F8NO4	585.30643	585.30644	0.004	-0.3438	
C24H43F4NO4	485.31282	485.31283	0.010	-0.3438	
C27H43F10NO4	635.30324	635.30320	-0.069	-0.3438	
C28H43F12NO4	685.30005	685.30005	-0.001	-0.3438	
C24H43F4NO5	501.30774	501.30774	0.001	-0.3398	$C_nH_{43}F_{2(n-22)}NO_5$
C26H43F8NO5	601.30135	601.30140	0.079	-0.3398	
C25H43F6NO5	551.30454	551.30454	-0.011	-0.3398	
C26H42F7NO4	565.30021	565.30020	-0.017	-0.3363	$C_nH_{42}F_{2(n-23)+1}NO_4$
C25H42F5NO4	515.30340	515.30341	0.013	-0.3363	
C27H42F9NO4	615.29701	615.29696	-0.091	-0.3363	
C25H41F6NO2	501.30415	501.30415	-0.004	-0.3362	$C_nH_{41}F_{2(n-22)}NO_2$
C26H41F8NO2	551.30095	551.30097	0.021	-0.3362	
C27H41F10NO2	601.29776	601.29773	-0.058	-0.3362	
C26H43F8NO6	617.29626	617.29625	-0.028	-0.3357	$C_nH_{43}F_{2(n-22)}NO_6$
C25H43F6NO6	567.29946	567.29946	-0.001	-0.3357	
C24H43F4NO6	517.30265	517.30263	-0.047	-0.3357	
C27H43F10NO6	667.29307	667.29302	-0.080	-0.3357	
C24H44ClF6NO2	527.29648	527.29646	-0.038	-0.3302	$C_nH_{44}ClF_{2(n-21)}NO_2$
C25H44ClF8NO2	577.29328	577.29332	0.059	-0.3302	
C27H44ClF12NO2	677.28690	677.28689	-0.013	-0.3302	
C26H44ClF10NO2	627.29009	627.29007	-0.036	-0.3302	
C26H40F7NO2	531.29473	531.29470	-0.057	-0.3287	$C_nH_{40}F_{2(n-23)+1}NO_2$
C25H40F5NO2	481.29792	481.29794	0.034	-0.3287	
C27H40F9NO2	581.29153	581.29163	0.161	-0.3287	
C26H41F8NO5	599.28570	599.28574	0.063	-0.3240	$C_nH_{41}F_{2(n-22)}NO_5$
C25H41F6NO5	549.28889	549.28893	0.062	-0.3240	
C24H41F4NO5	499.29209	499.29207	-0.039	-0.3240	
C26H39F6NO2	511.28850	511.28850	-0.004	-0.3212	$C_nH_{39}F_{2(n-23)}NO_2$
C25H39F4NO2	461.29169	461.29171	0.031	-0.3212	
C27H39F8NO2	561.28530	561.28532	0.021	-0.3212	
C28H39F10NO2	611.28211	611.28210	-0.024	-0.3212	
C29H39F12NO2	661.27892	661.27898	0.089	-0.3212	
C24H39F8NO4	557.27513	557.27511	-0.050	-0.3107	$C_nH_{39}F_{2(n-20)}NO_4$
C23H39F6NO4	507.27833	507.27834	0.017	-0.3107	
C25H39F10NO4	607.27194	607.27193	-0.023	-0.3107	
C22H39F4NO4	457.28152	457.28153	0.011	-0.3107	
C26H39F12NO4	657.26875	657.26870	-0.077	-0.3107	

4.6 Fingerprinting of PFASs

As for the discussion of PFAS identification, we will focus our fingerprinting analysis on the three samples highlighted above, only including known and unknown PFASs identified at Confidence Levels 1 and 2. Historically, fingerprinting of complex petroleum hydrocarbon and natural organic matter samples based on FT-ICR mass spectra has been performed using VKDs (van Krevelen 1950; Chen et al. 2016; Zito et al. 2020). Here, we modified the ordinate to illustrate the fluorine-to-carbon ratio in order to better represent PFAS species. Each dot in the diagram represents one identified species. As an example, perfluorohexane sulfonic acid (PFHxS, $C_6HF_{13}O_3S$) has a F/C ratio of 13/6 = 2.17 and an O/C ratio of 3/6 = 0.50.

Figure 10 shows a modified VKD of all PFAS identified in the AFFF sample at Confidence Levels 1 and 2, color-coded by relative abundance. PFOS was the most abundant species overall, while PFHxS was the second most abundant PFSA. The relative abundance of PFCAs was generally low, both for the deprotonated ions and the decarboxylated fragments (latter ones were filtered out and not included in this plot). The second most abundant species was $C_{11}H_3Cl_2F_{14}NO$. Note that relative abundances do not directly reflect absolute concentrations, but rather highlight similarities and differences between samples. The inherent difference in the ionization efficiency between different analytes or classes may obscure comparisons between relative concentrations (Hughey et al. 2004).

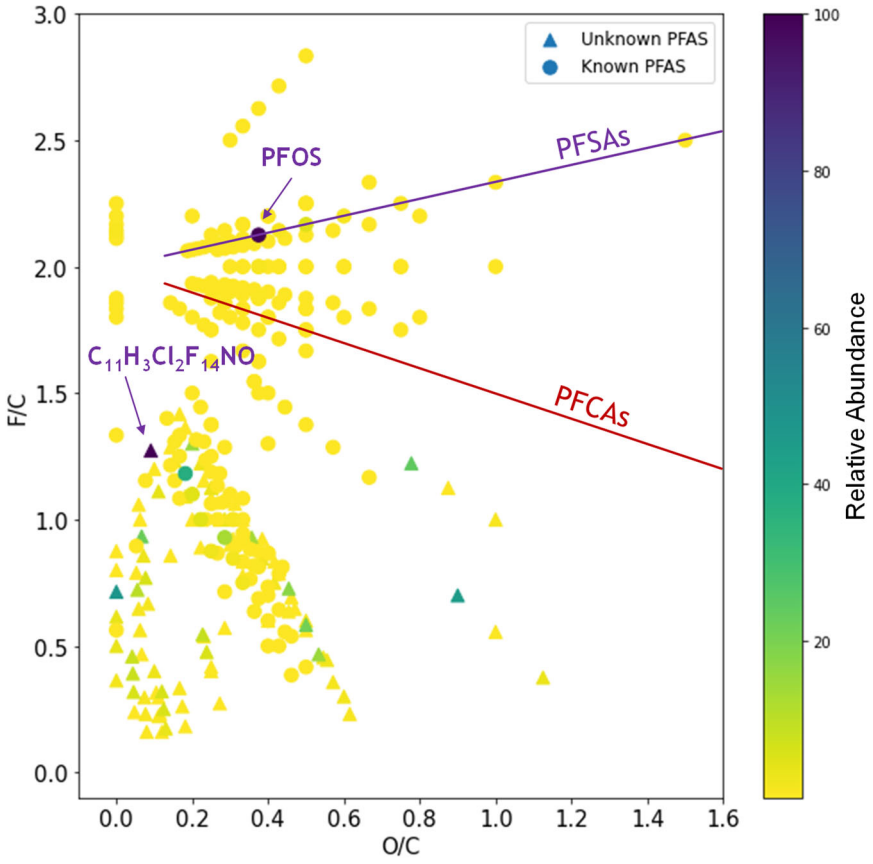

Figure 10: Modified van Krevelen diagram for the AFFF sample, highlighting the most abundant species as well as the lines on which PFSAs and PFCAs fall. Only PFASs identified at Confidence Levels 1 and 2 are shown.

Overall, the PFASs in the AFFF sample were distributed over a wide F/C range from <0.2 to >2.5, where pentafluorosulfanyl species exist. The majority of species had an O/C ratio <0.7. In contrast, the PFASs in the groundwater sample from Site B 1 showed an overall higher O/C ratio (Figure 11). While the original AFFF product(s) used at the site were not available to us, a higher O/C ratio would be expected during precursor transformation and possibly retardation along a groundwater flow path. Therefore, these modified VKDs may be very useful to illustrate fate and transport processes for complex PFAS mixtures.

As in the AFFF sample, PFOS was overall the most abundant species, followed by PFHxS among the PFAAs. The relative abundance of PFCAs was again low. The second most abundant species overall was $C_{10}H_7Cl_2F_7N_2O_9$.

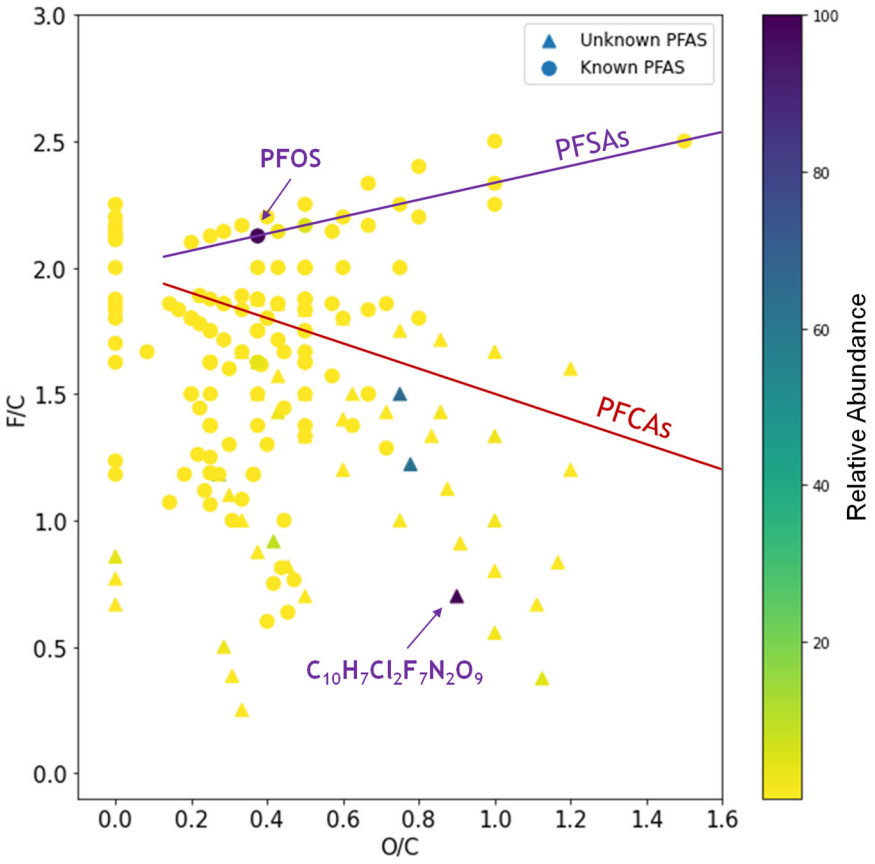

Figure 11: Modified van Krevelen diagram for the groundwater sample from Site B 1, highlighting the most abundant species as well as the lines on which PFSAs and PFCAs fall. Only PFASs identified at Confidence Levels 1 and 2 are shown.

Figure 12 shows the modified VKD for the WWTP effluent sample collected at Site B. Here, far less PFASs were detected as in the AFFF and groundwater samples, with the exception of PFBS all with an O/C ratio <0.6. While PFOS was again the most abundant species and PFCA had a relatively low abundance, a cluster of PFASs with F/C <0.5 and O/C <0.3 was very prominent, while absent in the groundwater sample. This cluster was composed of unique NO_x classes with >20 carbon atoms, $C_nH_{43}F_{2(n-22)}NO_4$ being the most abundant class.

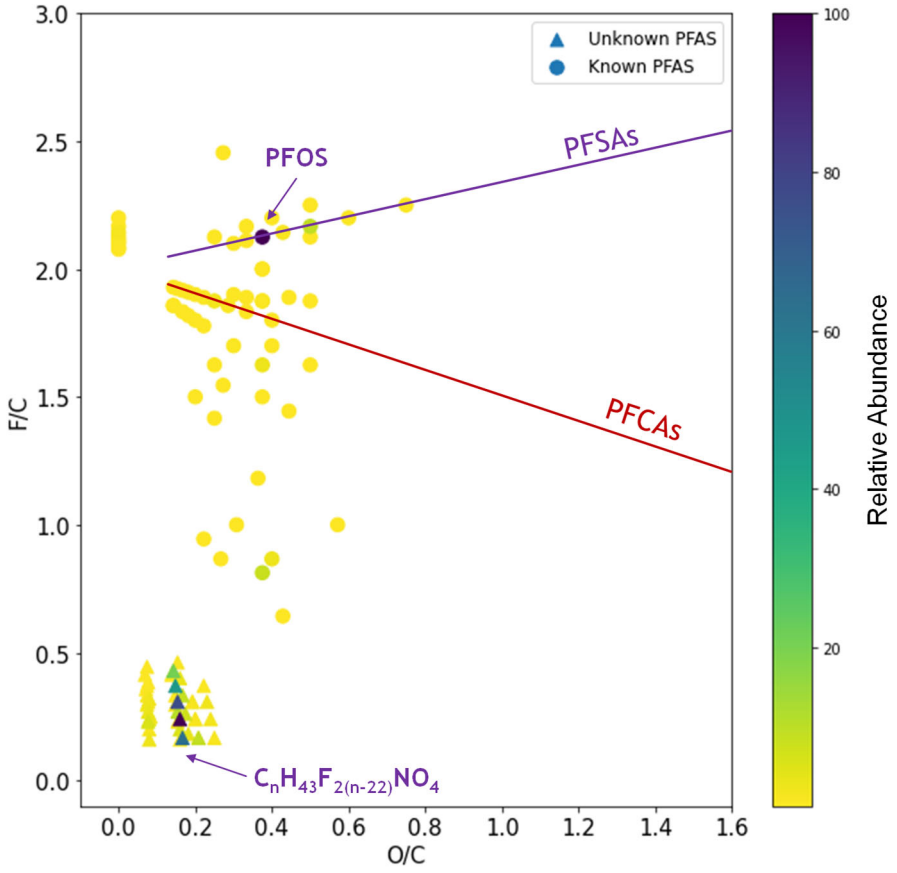

Figure 12: Modified van Krevelen diagram for the WWTP sample from Site B, highlighting the most abundant species as well as the lines on which PFSAs and PFCAs fall. Only PFASs identified at Confidence Levels 1 and 2 are shown.

An alternative option to fingerprint complex mixtures is by plotting the nominal oxidation state of carbon (NOSC) as a function of molecular weight, or analyte ion *m/z*. For natural organic matter, the NOSC value has been defined for a sulfur oxidation state of -II (LaRowe & Van Cappellen 2011). In most PFAS species such as sulfonic acids and sulfonamides, however, the sulfur oxidation state is +IV. Consequently, we have modified the NOSC value for PFASs as follows:

$$NOSC = 4 - \frac{4C - F + H - 2O + 4S - 3N - Cl + 5P}{C}$$

Figure 13 shows the plot of NOSC versus *m/z* for the AFFF sample. The identified PFASs range in NOSC from about -1.5 to 3 and cover a broad range from about 200 to 900 Da. In contrast, most identified PFASs in the groundwater sample fall in a much narrower range of 200 to just over 500 Da (Figure 14). This difference may be the result of retardation of more hydrophobic higher-molecular weight PFASs along the groundwater flow path. The WWTP effluent sample (Figure 15) is different from the other two samples through having less PFASs in the NOSC range of 0 to 1 but relatively more PFASs in the more reduced range around a NOSC value of -1, indicating a higher degree of carbon bonded to the less electronegative hydrogen.

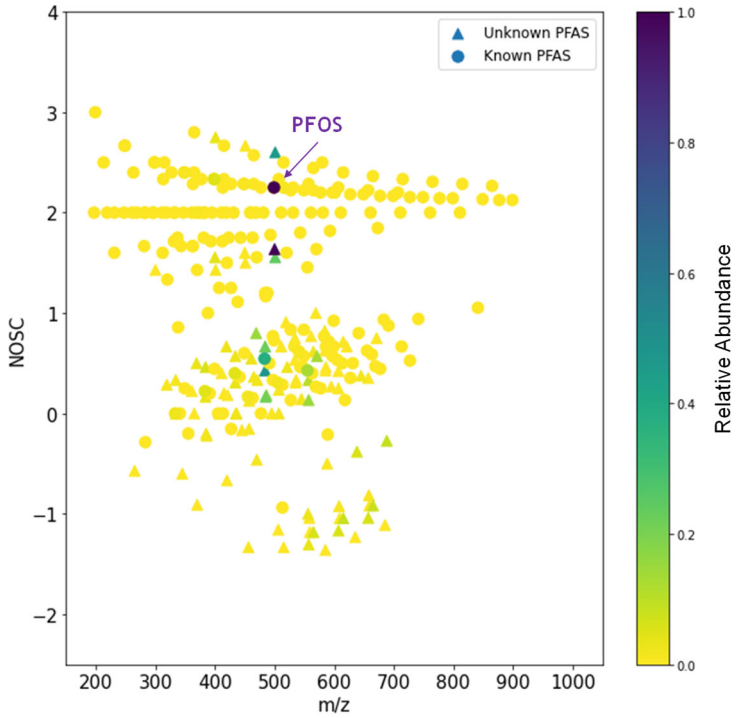

Figure 13: NOSC values as a function of *m/z* value for the AFFF sample. Only PFASs identified at Confidence Levels 1 and 2 are shown.

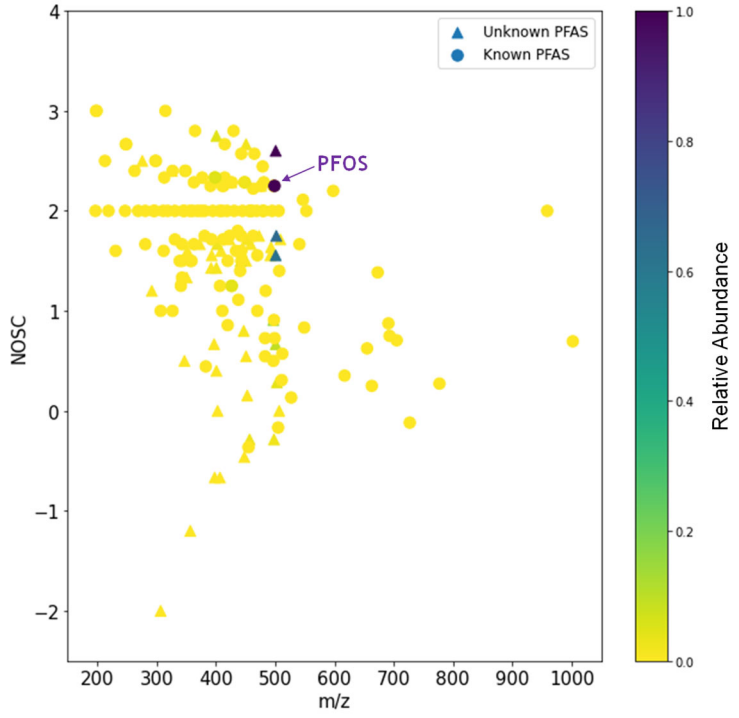

Figure 14: NOSC values as a function of *m/z* value for the groundwater sample from Site B 1. Only PFASs identified at Confidence Levels 1 and 2 are shown.

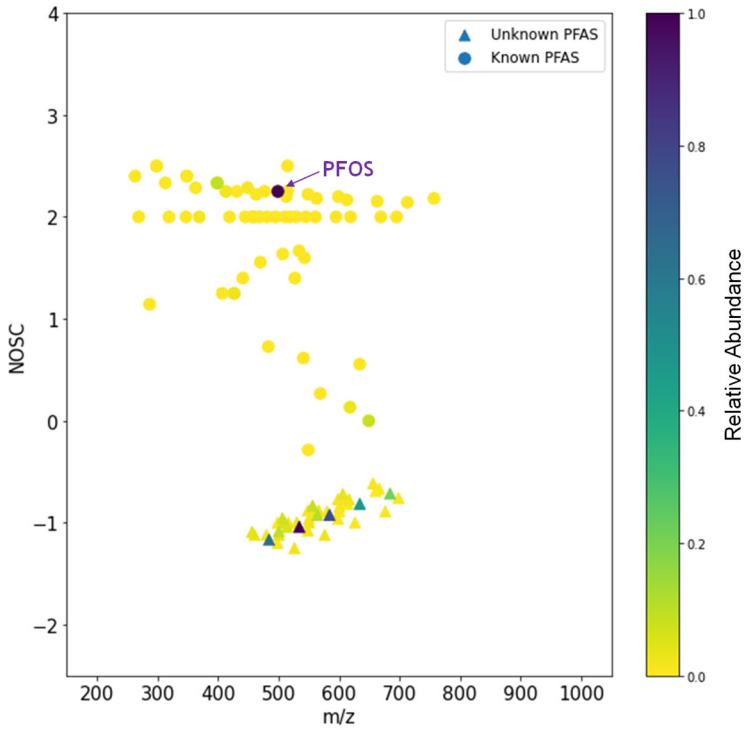

Figure 15: NOSC values as a function of *m/z* value for the WWTP sample from Site B. Only PFASs identified at Confidence Levels 1 and 2 are shown.

In conclusion, these three samples show very distinct fingerprints when plotted as modified VKDs or as NOSC versus *m/z*. Their variability in composition can be further interrogated for forensic purposes as shown below.

4.7 Forensic Analysis of PFASs

For forensic analysis including source zone allocation of complex solute mixtures such as petroleum hydrocarbons, PCA has been shown to be useful (Corilo et al. 2013; Barrow et al. 2015). PCA is a dimensionality reduction method that projects all data points onto the first few principal components to obtain lower-dimensional data while preserving a maximum of the data's variation. The input parameters used for PCA here were the abundances of known PFASs only, because the inclusion of the great number of unknowns (i.e., mostly precursors) with relatively little overlap between samples would have obscured a clear pattern.

Figure 16 shows the PCA for all collected samples combined. A clear separation of the AFFF sample from all other samples can be seen along the first principal component (x-axis), which accounts for 37.6% of the variability. While all Site A samples are clustered together, there is a clear separation between the groundwater and the WWTP samples from Site B as well as between the two groundwater samples from Site C along the second principal component (y-axis, 18.5% of explained variability). The latter observation may indicate impacts from different AFFF products used at Site C.

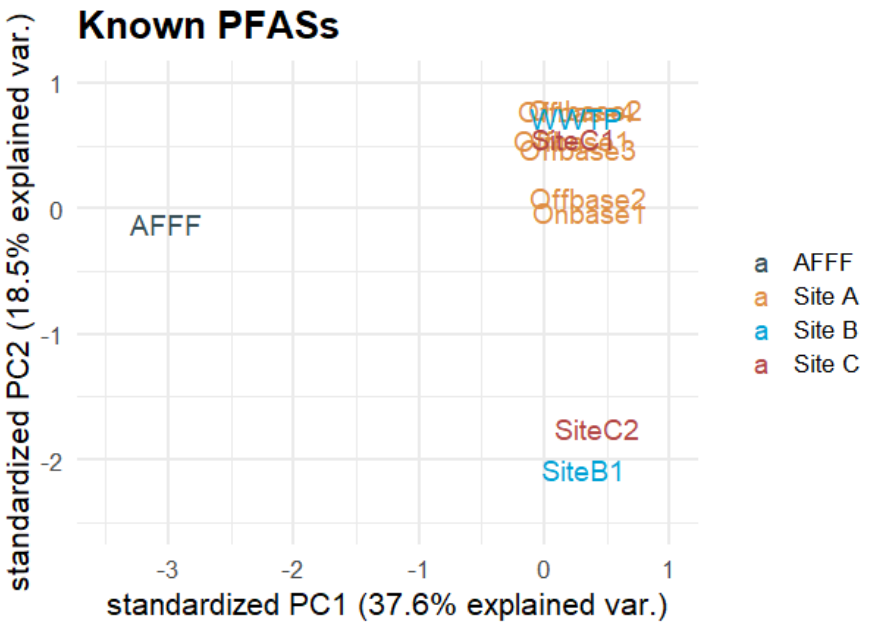

Figure 16: Principal component analysis for all analyzed samples.

To further analyze the variability between samples from Site A, a PCA was performed on these samples only. Figure 17 illustrates that the groundwater samples collected offbase (all upgradient of the site) are clearly clustered and separated in a different region of the diagram compared to the two onbase samples, indicating differences in PFAS composition and thus sources.

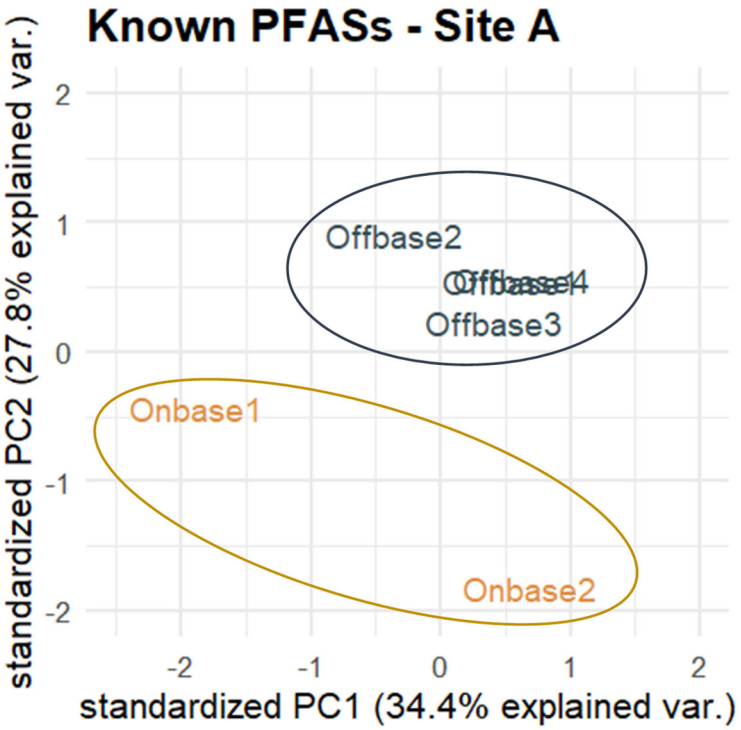

Figure 17: Principal component analysis for samples from Site A.

4.8 Identification of Potential Source-specific PFAS Markers

FT-ICR MS analysis is an exclusive, elaborate method, and instrument availability is highly limited. It is thus not suitable for routine sample analysis. Consequently, the final goal of our limited-scope project was to initiate the identification of product- or source-specific marker compounds. Our vision is that, once these analytes have been identified and validated through analysis on other mass spectrometric instruments, future analyses on widely and commercially used LC/MS-MS systems can target marker compounds for reliable and quantitative source zone allocation and other forensic purposes.

A first critical step in the identification of marker compounds is the separation into common and unique PFAS species, which is illustrated in the Venn diagrams in Figure 18. At Confidence Levels 1 and 2, this example revealed a total of 64 unique PFASs in the WWTP effluent sample (22 known and 42 unknown analytes) that were absent in the AFFF and groundwater samples. However, for an ultimate identification of source-specific marker compounds, more samples will have to be analyzed in the future to increase confidence in their uniqueness.

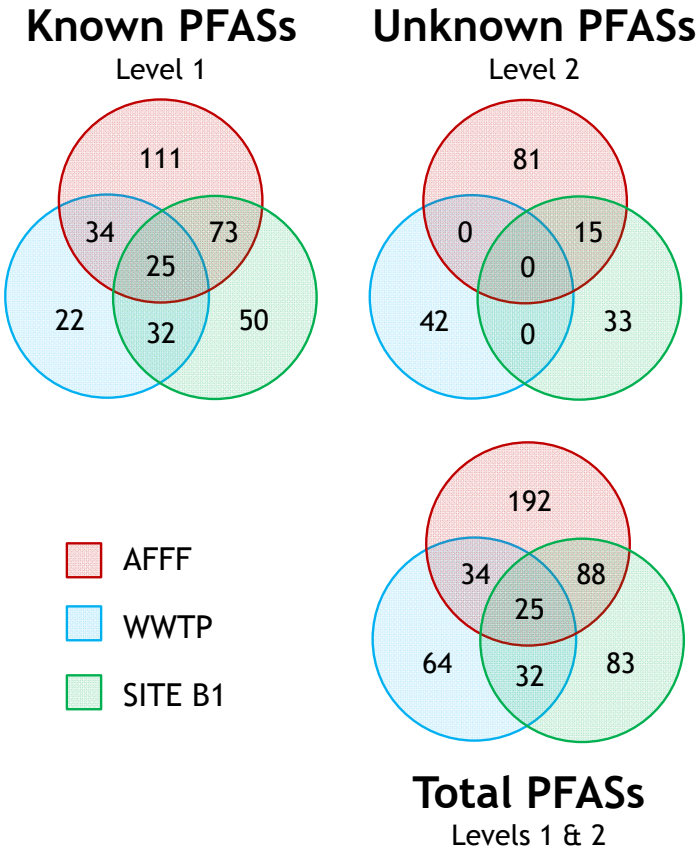

Figure 18: Venn diagrams for known, unknown, and total PFASs identified in the AFFF, Site B 1, and WWTP effluent samples, illustrating common and unique species. Only PFASs identified at Confidence Levels 1 and 2 are shown.

4.9 Mass Spectral Library

All PFAS species detected via ESI^- FT-ICR MS have been compiled and submitted as a mass spectral library along with this report. At Confidence Level 1 (known PFASs), 403 PFASs were identified in all samples combined. At Confidence Level 2, 300 novel PFASs were identified. At Confidence Levels 3 and 4, an additional 1739 and 6312 PFASs were detected, respectively.

The mass spectral library may serve as a molecular catalogue to accelerate future PFAS identification and AFFF fingerprinting activities. We hope to expand this list in the future through the analysis of additional samples, application of additional ionization modes (ESI^+ and $APPI^{+/-}$), and information on fragments generated by ultrahigh-resolution tandem MS^n experiments that will further add confidence to the molecular formula assignments (Figure 9).

4.10 Quality Assurance (QA) and Quality Control (QC)

In contrast to quantitative analytical approaches such as LC/QQQ-MS, FT-ICR MS is a qualitative technique. Consequently, QA/QC measures will be different and, in fact, have to be established. As this is a method development project for a novel PFAS analytical approach, acceptance criteria for sample preparation recovery, accuracy, precision, and background contamination are not defined upfront but will eventually be an outcome of this development, guiding future FT-ICR MS-based analyses. Furthermore, the development of a Standard Reference Material would be particularly helpful to aid in mass spectral calibration.

As described in Chapter 3, several procedures were undertaken to ensure accurate and reliable measurements, minimizing effects of potential background contamination. However, as the data analysis of an FT-ICR mass spectrum takes several weeks, a complete check for PFAS contamination cannot be performed during sample batch analysis. Only PFAS-free materials and solvents were used (as verified by our own LC/QQQ-MS analyses). The FT-ICR MS was extensively cleaned between samples, and its cleanliness was verified prior to sample analysis by first analyzing ultrahigh-purity solvent. Nevertheless, 43 PFASs were detected in the travel blank (T) and 45 PFASs were detected in the field blank (T). 30 of the PFASs found in the field blank were also found in the travel blank. Yet, our LC/QQQ-MS analyses had not detected any of the 24 PFASs listed in Table A 1 (Appendix A) above the respective quantification limits (5-10 ng/L). Two possible explanations exist for these detects, and future analyses should be performed to clarify the source of these detects: (1) Even extensive rinsing of the instrument between samples did not fully remove accumulated PFASs, causing analyte carryover. (2) The FT-ICR MS is an ion trap, in which ionized analytes are accumulated until a sufficiently strong signal is achieved. This is in contrast to other mass spectrometry-based techniques such as LC/QQQ-MS or LC/QTOF-MS, where a fixed sample volume is injected. Consequently, it seems possible that PFASs were accumulated in the ion trap to a detectable extent while being at a concentration below LC/QQQ-MS quantification limit in the original sample. This conclusion is supported by the fact that PFOS was the major species with a relative abundance of 100 in most analyzed samples (Figures A 1-3), while its relative abundance was 0.015 in the travel blank and 0.046 in the field blank, whose spectra were dominated by DOM species. In other words, the largest peaks in the two blanks were several thousand times larger than the PFOS peaks after trapping enough ions for analysis.

The accuracy of our FT-ICR mass measurements was quantified as mean parts per million (ppm) error according to Brenton & Godfrey (2010):

$$\Delta m_i = \frac{m_i - m_a}{m_a}$$

where m_i is the measured accurate mass (Da) and m_a is the theoretical exact mass (Da). Precision was evaluated through the standard ppm error. Figure 19 through Figure 21 show the ppm errors for PFSAs in the three highlighted samples. All ppm errors fall within a range of ±0.17 ppm.

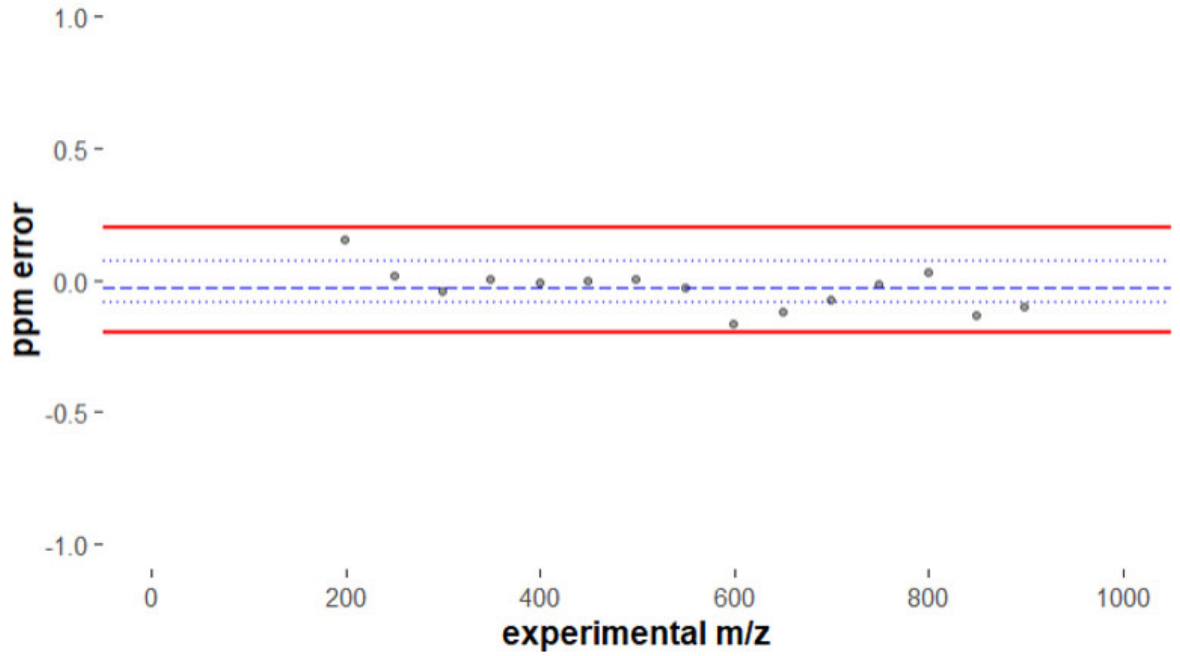

MF <chr>	theor_mass <dbl>	exper_mz <dbl>	ppm_error <dbl>
C2HF5O3S	199.95666	198.94941	0.1541684116
C3HF7O3S	249.95346	248.94619	0.0177112970
C4HF9O3S	299.95027	298.94298	-0.0399166170
C5HF11O3S	349.94707	348.93980	0.0046492745
C6HF13O3S	399.94388	398.93660	-0.0119341742
C7HF15O3S	449.94069	448.93341	-0.0026070103
C8HF17O3S	499.93749	498.93022	0.0048546071
C9HF19O3S	549.93430	548.92701	-0.0254084897
C10HF21O3S	599.93111	598.92373	-0.1673075439
C11HF23O3S	649.92791	648.92056	-0.1181254082

Figure 19: Molecular formulas, theoretical neutral masses, negative ion-ESI measured masses, and ppm mass errors for PFSAs in the AFFF sample. The red lines indicate ±0.2 ppm error used as cutoff for formula assignment.

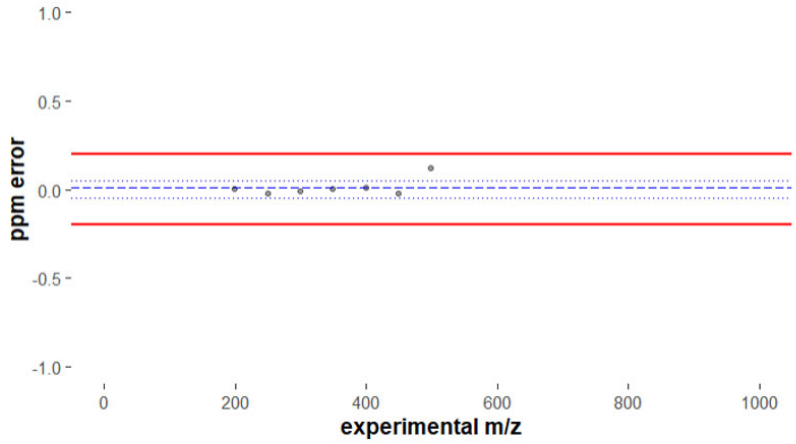

MF <chr>	theor_mass <dbl>	exper_mz <dbl>	ppm_error <dbl>
C2HF5O3S	199.95666	198.94938	0.0041358962
C3HF7O3S	249.95346	248.94618	-0.0222961505
C4HF9O3S	299.95027	298.94299	-0.0065777569
C5HF11O3S	349.94707	348.93980	0.0046492745
C6HF13O3S	399.94388	398.93661	0.0130693337
C7HF15O3S	449.94069	448.93340	-0.0248321618
C8HF17O3S	499.93749	498.93028	0.1248696103

Figure 20: Molecular formulas, theoretical neutral masses, negative ion-ESI measured masses, and ppm mass errors for PFSAs in the groundwater sample from Site B 1. The red lines indicate ±0.2 ppm error used as cutoff for formula assignment.

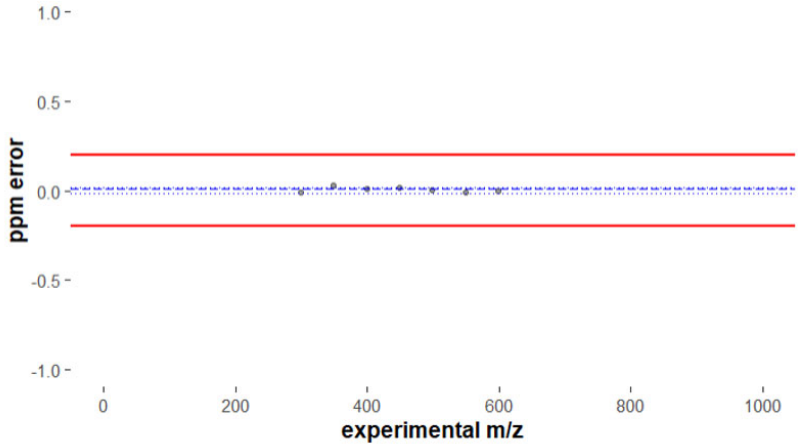

MF <chr>	theor_mass <dbl>	exper_mz <dbl>	ppm_error <dbl>
C4HF9O3S	299.95027	298.94299	-0.00657775687
C5HF11O3S	349.94707	348.93981	0.03322502426
C6HF13O3S	399.94388	398.93661	0.01306933367
C7HF15O3S	449.94069	448.93342	0.01961814143
C8HF17O3S	499.93749	498.93022	0.00485460705
C9HF19O3S	549.93430	548.92702	-0.00722449944
C10HF21O3S	599.93111	598.92383	-0.00062173811

Figure 21: Molecular formulas, theoretical neutral masses, negative ion-ESI measured masses, and ppm mass errors for PFSAs in the WWTP effluent sample. The red lines indicate ±0.2 ppm error used as cutoff for formula assignment.

Table 5 shows the mean and standard ppm errors for all known PFASs detected in the samples. Overall, the average error achieved was 0.0075 ± 0.0579 ppm. These metrics clearly show the resolving power of the 21 tesla FT-ICR MS, unmatched by any other mass spectrometric technique.

Table 5: Mean ppm error (accuracy) and standard ppm error (precision) for all known PFASs detected via FT-ICR MS.

Location	Sample ID	Mean ppm error	Std. ppm error
N/A	AFFF	-0.0180	0.0601
Site A	ONBASE 1	0.0024	0.0489
	ONBASE 2	-0.0031	0.0566
	OFFBASE 1	-0.0011	0.0630
	OFFBASE 2	0.0135	0.0534
	OFFBASE 3	0.0215	0.0657
	OFFBASE 4	0.0079	0.0613
SITE B	SITE B 1	-0.0031	0.0618
	WWTP	-0.0007	0.0407
SITE C	SITE C 1	0.0414	0.0679
	SITE C 2	0.0215	0.0569
AVERAGE		0.0075	0.0579

5 CONLUSIONS AND IMPLICATIONS FOR FUTURE RESEARCH

The developmental work performed in this one-year limited scope project clearly demonstrates the unmatched capabilities of FT-ICR MS for the identification of complex PFAS mixtures via ultrahigh mass resolving power and mass accuracy, revealing molecular features that would remain unresolved on lower-performance instruments. Here, we discovered 300 new PFAS species and 75 novel classes at the highest confidence level with thousands more to be validated. Moreover, we demonstrated how these data can be used in the future for PFAS identification, sample fingerprinting, forensic analysis, and identification of source-specific marker compounds.

While this work is a major advancement in the identification of PFASs and forensic analysis, several tasks remain to be performed in order to take full advantage of the instrument's full capabilities:

1) As shown in Table 1, thousands of peaks remain unassigned, neither being identified as DOM by PetroOrg® nor as PFASs through our spectral processing. While some of these peaks may be fragments, isotopologues, or background contamination, it is certainly possible that some PFASs did not pass our stringent identification criteria such as ±0.1 ppm mass error.

2) Our analyses in this report focus on species ionizable in negative ESI. Additional steps for processing positive-ion spectra will need to be developed and are challenged by the occurrence of multiple adducts (i.e., protonated, ammoniated, sodiated, etc.). For groundwater forensics, negative ESI may be sufficient as negatively charged species typically dominate the PFAS composition in a downgradient plume. However, for tasks such as AFFF characterization or soil analysis, the development of a positive ESI workflow would be valuable.

3) Even though a low average error of 0.0075 ± 0.0579 ppm was achieved for known PFASs, a larger number of commercially available PFAS standards (or "reference material") would be helpful for the calibration of PFAS spectra (Savory et al. 2011).

4) To add further lines of evidence, and thus confidence, to our formula assignments, MS^n fragmentation and possibly chromatographic separation may be attempted in future experiments.

5) The source of PFAS detections in the blanks, even though at low abundances, needs to be addressed. Likely, specific instrument cleaning protocols need to be developed for the analysis of PFAS samples.

6) To expand our mass spectral library, more samples need to be analyzed, especially AFFF products and common alternative PFAS sources such as WWTP effluent and landfill leachate. A larger, more representative database for each of these sources will enable the identification of source-specific marker compounds and improve sample fingerprinting. Furthermore, groundwater sampling at higher spatial resolution and along a known direction of groundwater flow will enable more accurate conclusions regarding source allocation.

7) Newly discovered PFASs should be validated through additional QTOF or Orbitrap analyses including chromatographic separation and fragmentation.

8) Ultimately, the analysis of identified product- or source-specific marker compounds needs to be transferred to more accessible, commercial LC/MS-MS systems.

Collectively, this first-of-its-kind application of FT-ICR MS and the workflow developed here are a critical first step in cataloguing PFASs associated with AFFF and non-AFFF sources as well as in identifying unique marker compounds for fingerprinting that can be targeted in the future on more widely accessible mass spectrometric instruments. Ultimately, this information will provide critical guidance to DoD remedial program managers (1) to track transformation and retardation processes of AFFFs, (2) to date plumes, (3) to understand the extent of PFAS contamination, and (4) to determine the potential liability associated with past releases.

6 LITERATURE CITED

Ahrens, L.; Harner, T.; Shoeib, M.; Lane, D.A.; Murphy, J.G. Improved characterization of gas–particle partitioning for per-and polyfluoroalkyl substances in the atmosphere using annular diffusion denuder samplers. *Environmental Science & Technology* **2012**, 46: 7199-7206.

Allred, B.M.; Lang, J.R.; Barlaz, M.A.; Field, J.A. Orthogonal zirconium diol/C18 liquid chromatography–tandem mass spectrometry analysis of poly and perfluoroalkyl substances in landfill leachate. *J. Chromatogr. A* **2014**, 1359: 202-211.

Backe, W.J.; Day, T.C.; Field, J.A. Zwitterionic, cationic, and anionic fluorinated chemicals in aqueous film forming foam formulations and groundwater from US military bases by nonaqueous large-volume injection HPLC-MS/MS. *Environmental Science & Technology* **2013**, 47: 5226-5234.

Barrow, M.P.; Peru, K.M.; Fahlman, B.; Hewitt, L.M.; Frank, R.A.; Headley, J.V. Beyond Naphthenic Acids: Environmental Screening of Water from Natural Sources and the Athabasca Oil Sands Industry Using Atmospheric Pressure Photoionization Fourier Transform Ion Cyclotron Resonance Mass Spectrometry. *J. Am. Soc. Mass Spectrom.* **2015**, 26:1508-1521.

Barton, C.A.; Butler, L.E.; Zarzecki, C.J.; Flaherty, J.; Kaiser, M. Characterizing perfluorooctanoate in ambient air near the fence line of a manufacturing facility: comparing modeled and monitored values. *Journal of the Air & Waste Management Association 2006*, 56: 48-55.

Barzen-Hanson, K.A.; Roberts, S.C.; Choyke, S.; Oetjen, K.; McAlees, A.; Riddell, N.; McCrindle, R.; Ferguson, P.L.; Higgins, C.P.; Field, J.A. Discovery of 40 classes of per-and polyfluoroalkyl substances in historical aqueous film-forming foams (AFFFs) and AFFF-impacted groundwater. *Environmental Science & Technology* **2017**, 51: 2047-2057.

Blakney, G. T.; Hendrickson, C. L.; Marshall, A. G. Predator data station: A fast data acquisition system for advanced FT-ICR MS experiments. *Int. J. Mass Spectrom.* **2011,** 306: 246-252.

Boldin, I. A.; Nikolaev, E. N. Fourier transform ion cyclotron resonance cell with dynamic harmonization of the electric field in the whole volume by shaping of the excitation and detection electrode assembly. *Rapid Commun. Mass Spectrom.* **2011**, 25: 122-126.

Brändli, R.C.; Kupper, T.; Bucheli, T.D.; Zennegg, M.; Huber, S.; Ortelli, D.; Müller, J.; Schaffner, C.; Iozza, S.; Schmid, P. Organic pollutants in compost and digestate. Part 2. Polychlorinated dibenzo-p-dioxins, and-furans, dioxin-like polychlorinated biphenyls, brominated flame retardants, perfluorinated alkyl substances, pesticides, and other compounds. *Journal of Environmental Monitoring* **2007**, 9: 465-472.

Brenton, A.G.; Godfrey, A.R. Accurate Mass Measurement: Terminology and Treatment of Data. *J. Am. Soc. Mass. Spectrom.* **2010**, 21: 1821-1835.

Brusseau, M.L.; Anderson, R.H.; Guo, B. PFAS concentrations in soils: Background levels versus contaminated sites. *Science of The Total Environment* **2020**, 740: 140017.

Buck, R.C.; Franklin, J.; Berger, U.; Conder, J.M.; Cousins, I.T.; De Voogt, P.; Astrup Jensen, A.; Kannan, K.; Mabury, S.A.; van Leeuwen, S.P.J. Perfluoroalkyl and polyfluoroalkyl substances in the environment: terminology, classification, and origins. *Integrated Environmental Assessment and Management* **2011**, 7: 513-541.

Chen, T.; Beu, S. C.; Kaiser, N. K.; Hendrickson, C. L., Note: Optimized circuit for excitation and detection with one pair of electrodes for improved Fourier transform ion cyclotron resonance mass spectrometry. *Rev. Sci. Instrum.* **2014,** 85: 0666107/1-066107/3.

Chen, H.; Hou, A.; Corilo, Y.E.; Lin, Q.; Lu, J.; Mendelssohn, I.A.; Zhang, R.; Rodgers, R.P.; McKenna, A.M. 4 Years after the Deepwater Horizon Spill: Molecular Transformation of Macondo Well Oil in Louisiana Salt Marsh Sediments Revealed by FT-ICR Mass Spectrometry. *Environmental Science & Technology* **2016**, 50: 9061-9069.

Chen, H.; Yao, Y.; Zhao, Z.; Wang, Y.; Wang, Q.; Ren, C.; Wang, B.; Sun, H.; Alder, A.C.; Kannan, K. Multimedia distribution and transfer of per-and polyfluoroalkyl substances (PFASs) surrounding two fluorochemical manufacturing facilities in Fuxin, China. *Environmental Science & Technology* **2018**, 52: 8263-8271.

Corilo, Y.E.; Podgorski, D.C.; McKenna, A.M.; Lemkau, K.L.; Reddy, C.M.; Marshall, A.G.; Rodgers, R.P. Oil Spill Source Identification by Principal Component Analysis of Electrospray Ionization Fourier Transform Ion Cyclotron Resonance Mass Spectra. *Analytical Chemistry* **2013**, 85: 9064-9069.

Corilo, Y. E. *PetroOrg Software*, Florida State University, Omics LLC: Tallahassee, FL, 2014.

D'Agostino, L.A.; Mabury, S.A. Identification of Novel Fluorinated Surfactants in Aqueous Film Forming Foams and Commercial Surfactant Concentrates. *Environ. Sci. Technol.* **2014**, *48*, 121-129.

Ellis, D.A.; Martin, J.W.; Mabury, S.A.; Hurley, M.D.; Sulbaek Andersen, M.P.; Wallington, T.J. Atmospheric lifetime of fluorotelomer alcohols. *Environmental Science & Technology* **2003**, 37: 3816-3820.

Ellis, D.A.; Martin, J.W.; De Silva, A.O.; Mabury, S.A.; Hurley, M.D.; Sulbaek Andersen, M.P.; Wallington, T.J. Degradation of fluorotelomer alcohols: a likely atmospheric source of perfluorinated carboxylic acids. *Environmental Science & Technology* **2004**, 38: 3316-3321.

Emmett, M. R.; White, F. M.; Hendrickson, C. L.; Shi, S. D.-H.; Marshall, A. G., Application of micro-electrospray liquid chromatography techniques to FT-ICR MS to enable high-sensitivity biological analysis. *J. Am. Soc. Mass Spectrom.* **1998,** 9: 333-340.

Fang, X.; Wang, Q.; Zhao, Z.; Tang, J.; Tian, C.; Yao, Y.; Yu, J.; Sun, H. .Distribution and dry deposition of alternative and legacy perfluoroalkyl and polyfluoroalkyl substances in the air above the Bohai and Yellow Seas, China. *Atmospheric Environment* **2018**, 192: 128-135.

Fernandes, A.R.; Lake, I.R.; Dowding, A.; Rose, M.; Jones, N.R.; Petch, R.; Smith, F.; Panton, S. The potential of recycled materials used in agriculture to contaminate food through uptake by livestock. *Science of the Total Environment* **2019**, 667: 359-70.

Filipovic, M.; Berger, U. Are perfluoroalkyl acids in waste water treatment plant effluents the result of primary emissions from the technosphere or of environmental recirculation? *Chemosphere* **2015**, 129: 74-80.

Galloway, J.E.; Moreno, A.V.P; Lindstrom, A.B.; Strynar, M.J.; Newton, S.; May, A.A.; Weavers, L.K. Evidence of Air Dispersion: HFPO–DA and PFOA in Ohio and West Virginia Surface Water and Soil near a Fluoropolymer Production Facility. *Environmental science & technology* **2020**, 54: 7175-7184.

García, R.A.; Chiaia-Hernandez, A.C.; Lara-Martin, P.A.; Loos, M.; Hollender, J.; Oetjen, K.; Higgins, C. P.; Field, J.A. Suspect Screening of Hydrocarbon Surfactants in AFFFs and AFFFContaminated Groundwater by High-Resolution Mass Spectrometry. *Environ. Sci. Technol.* **2019**, 53: 8068-8077.

Gobelius, L.; Lewis, J.; Ahrens, L. Plant uptake of per-and polyfluoroalkyl substances at a contaminated fire training facility to evaluate the phytoremediation potential of various plant species. *Environmental Science & Technology* **2017**, 51: 12602-12610.

Gottschall, N.; Topp, E.; Edwards, M.; Payne, M.; Kleywegt, S.; Lapen, D.R. Brominated flame retardants and perfluoroalkyl acids in groundwater, tile drainage, soil, and crop grain following a high application of municipal biosolids to a field. *Science of The Total Environment* **2017**, 574: 1345-1359.

Gribble, M.O.; Bartell, S.M.; Kannan, K.; Wu, Q.; Fair, P.A.; Kamen, D.L. Longitudinal measures of perfluoroalkyl substances (PFAS) in serum of Gullah African Americans in South Carolina: 2003–2013. *Environmental Research* **2015**, 143: 82-88.

Guelfo, J.L.; Marlow, T.; Klein, D.M.; Savitz, D.A.; Frickel, S.; Crimi, M.; Suuberg, E.M. Evaluation and management strategies for per-and polyfluoroalkyl substances (PFASs) in drinking water aquifers: perspectives from impacted US Northeast communities. *Environmental Health Perspectives* **2018**, 126: 065001.

Gueneli, N.; McKenna, A. M.; Ohkouchi, N.; Boreham, C. J.; Beghin, J.; Javaux, E. J.; Brocks, J. J. (2018): 1.1 Billion Years Old Porphyrins Establish a Marine Ecosystem Dominated by Bacterial Primary Producers. *Proceedings of the National Academy of Sciences* **2018**, 115: E6978-E6986.

Hamid, H.; Li, L.Y.; Grace, J.R. Review of the fate and transformation of per- and polyfluoroalkyl substances (PFASs) in landfills. *Environmental Pollution* **2018**, 235: 74-84.

He, H. (2009). *Electrospray Ionization Fourier Transform Ion Cyclotron Resonance Mass Spectrometry in Biological Applications: Lipids and Proteins* (Master's thesis). Florida State University Libraries.

Hendrickson, C. L.; Quinn, J. P.; Kaiser, N. K.; Smith, D. F.; Blakney, G. T.; Chen, T.; Marshall, A. G.; Weisbrod, C. R.; Beu, S. C., 21 Tesla Fourier transform ion cyclotron resonance mass spectrometer: A national resource for ultrahigh resolution mass analysis. *J. Am. Soc. Mass Spectrom.* **2015,** 26: 1626-1632.

Houtz, E.F.; Higgins, C.P.; Field, J.A.; Sedlak, D.L. Persistence of perfluoroalkyl acid precursors in AFFF-impacted groundwater and soil. *Environmental Science & Technology* **2013**, 47: 8187-8195.

Houtz, E.F.; Sutton, R.; Park, J.-S.; Sedlak, M. Poly-and perfluoroalkyl substances in wastewater: Significance of unknown precursors, manufacturing shifts, and likely AFFF impacts. *Water Research* **2016**, 95: 142-149.

Hu, X.C.; Dassuncao, C.; Zhang, X.; Grandjean, P.; Weihe, P.; Webster, G.M.; Nielsen, F.; Sunderland, E.M. Can profiles of poly-and Perfluoroalkyl substances (PFASs) in human serum provide information on major exposure sources? *Environmental Health* **2018**, 17: 11.

Hughey, C. A.; Hendrickson, C. L.; Rodgers, R. P.; Marshall, A. G.; Qian, K., Kendrick Mass Defect Spectroscopy: A Compact Visual Analysis for Ultrahigh-Resolution Broadband Mass Spectra. *Anal. Chem.* **2001,** *73*, 4676-4681.

Hughey, C. A.; Rodgers, R. P.; Marshall, A. G.; Walters, C. C.; Qian, K.; Mankiewicz, P. Acidic and neutral polar NSO compounds in Smackover oils of different thermal maturity revealed by electrospray high field Fourier transform ion cyclotron resonance mass spectrometry. *Org. Geochem.* **2004**, 35: 863-880.

Huset, C.A., Barlaz, M.A., Barofsky, D.F., Field, J.A. Quantitative determination of fluorochemicals in municipal landfill leachates. *Chemosphere* **2011**, 82: 1380-1386.

Jakobsson, K.; Diab, K.K.; Lindh, C.; Persson, B.; Jönsson, B. Exponering för perfluorerade ämnen (PFAS) i dricksvatten i Ronneby kommun. *Report*, 8: 2014.

Jiang, T. (2017). Top-down and Middle-down Proteomics by Fourier Transform Ion Cyclotron Resonance Mass Spectrometry (Master's thesis). Florida State University Libraries.

Kaiser, N.K.; McKenna, A.M.; Savory, J.J.; Hendrickson, C.L.; Marshall, A.G. Tailored ion radius distribution for increased dynamic range in FT-ICR mass analysis of complex mixtures. *Anal. Chem.* **2013,** 85: 265-272.

Kendrick, E. A mass scale based on CH_2 = 14.0000 for high resolution mass spectrometry of organic compounds. *Anal. Chem.* **1963,** 35: 2146-2154.

Kibbey, T.C.G.; Jabrzemski, R.; O'Carroll, D.M. Supervised machine learning for source allocation of per- and polyfluoroalkyl substances (PFAS) in environmental samples. *Chemosphere* **2020**, 252: 126593.

Koch, A.; Kärrman, A.; Yeung, L.W.Y.; Jonsson, M.; Ahrens, L.; Wang, T. Point source characterization of per-and polyfluoroalkyl substances (PFASs) and extractable organofluorine (EOF) in freshwater and aquatic invertebrates. *Environmental Science: Processes & Impacts* **2019**, 21: 1887-1898.

Krepich, S. Per- and Polyfluorinated Alkylsubstances (PFAS) from Dairy and Fish Using QuEChERS, SPE, and LC-MS/MS. *The Column* **2019**, 15 (9): 30.

Lang, J. R.; McKay Allred, B.; Peaslee, G. F.; Field, J. A.; Barlaz, M. A. Release of Per- and Polyfluoroalkyl Substances (PFASs) from Carpet and Clothing in Model Anaerobic Landfill Reactors. *Environ. Sci. Technol.* **2016**, 50: 5024-5032.

Lang, J.R.; Allred, B.M.; Field, J.A.; Levis, J.W.; Barlaz, M.A. National estimate of per-and polyfluoroalkyl substance (PFAS) release to US municipal landfill leachate. *Environ. Sci. Technol.* **2017**, 51: 2197-2205.

LaRowe, D.E.; Van Cappellen, P. Degradation of natural organic matter: A thermodynamic analysis. *Geochimica et Cosmochimica Acta* **2011**, 75: 2030-2042.

Lazcano, R.K.; Choi, Y.J.; Mashtare, M.L.; Lee, L.S. Characterizing and Comparing Per- and Polyfluoroalkyl Substances in Commercially Available Biosolid and Organic Non-Biosolid-Based Products. *Environ. Sci. Technol.* **2020**, 54: 8640-8648.

Leefmann, T.; Frickenhaus, S.; Koch, B. P. UltraMassExplorer - a browser-based application for the evaluation of high-resolution mass spectrometric data. *Rapid Communications in Mass Spectrometry* **2019**, 33: 193-202.

Lobodin, V.V.; Juyal, P.; McKenna, A.M.; Rodgers, R.P.; Marshall, A.G. Tetramethylammonium hydroxide as a reagent for complex mixture analysis by negative ion electrospray ionization mass spectrometry. *Analytical Chemistry* **2013**, 85: 7803-7808.

Marshall, A. G.; Hendrickson, C. L.; Jackson, G. S. Fourier transform ion cyclotron resonance mass spectrometry: A primer. *Mass Spectrom. Rev.* **1998**, 17: 1-35.

McKenna, A. M.; Williams, J. T.; Putman, J. C.; Aeppli, C.; Reddy, C. M.; Valentine, D. L.; Lemkau, K. L.; Kellermann, M. Y.; Savory, J. J.; Kaiser, N. K.; Rodgers, R. P.; Marshall, A. G. Unprecedented Ultrahigh Resolution FT-ICR Mass Spectrometry and Parts-Per-Billion Mass Accuracy Enable Direct Characterization of Nickel and Vanadyl Porphyrins in Petroleum from Natural Seeps. *Energy & Fuels* **2014**, 28: 2454-2464.

McLafferty, F. W.; Turecek, F. *Interpretation of Mass Spectra, 4th ed.* University Science Books: Mill Valley, CA, 1993.

Mejia-Avendaño, S.; Munoz, G.; Duy, S.V.; Desrosiers, M.; Benoît, P.; Sauvé, S.; Liu, J. Novel fluoroalkylated surfactants in soils following firefighting foam deployment during the Lac-Megantic railway accident. *Environmental Science & Technology* **2017**, 51: 8313-8323.

Milinovic, J.; Lacorte, S.; Rigol, A.; Vidal, M. Sorption of perfluoroalkyl substances in sewage sludge. *Environmental Science and Pollution Research* **2016**, 23: 8339-8348.

Milley, S.A.; Koch, I.; Fortin, P.; Archer, J.; Reynolds, D.; Weber, K.P. 'Estimating the number of airports potentially contaminated with perfluoroalkyl and polyfluoroalkyl substances from aqueous film forming foam: A Canadian example. *Journal of Environmental Management* **2018**, 222: 122-31.

Nickerson, A.; Maizel, A.C.; Kulkarni, P.R.; Adamson, D.T.; Kornuc, J.J.; Higgins, C.P. Enhanced extraction of AFFF-associated PFASs from source zone soils. *Environmental Science & Technology* **2020**, 54: 4952-4962.

Nzeribe, B.N.; Crimi, M.; Mededovic Thagard, S.; Holsen, T.M. Physico-Chemical Processes for the Treatment of Per-And Polyfluoroalkyl Substances (PFAS): A review. *Critical Reviews in Environmental Science and Technology* **2019**, 49: 866-915.

Organisation for Economic Co-operation and Development. 2021. Comprehensive Global Database of Per- and Polyfluoroalkyl Substances. http://www.oecd.org/chemicalsafety/portal-perfluorinated-chemicals/. Accessed 04/04/2021.

Park, M.; Wu, S.; Lopez, I.J.; Chang, J.Y.; Karanfil, T.; Snyder, S.A. Adsorption of perfluoroalkyl substances (PFAS) in groundwater by granular activated carbons: Roles of hydrophobicity of PFAS and carbon characteristics. *Water Research* **2020**, 170: 115364.

Piekarz, A.M.; Primbs, T.; Field, J.A.; Barofsky, D.F.; Simonich, S. Semivolatile fluorinated organic compounds in Asian and western US air masses. *Environmental Science & Technology* **2007**, 41: 8248-8255.

Place, B.J.; Field, J.A. Identification of novel fluorochemicals in aqueous film-forming foams used by the US military. *Environmental Science & Technology* **2012**, 46: 7120-7127.

Rankin, K.; Mabury, S.A.; Jenkins, T.M.; Washington, J.W. A North American and global survey of perfluoroalkyl substances in surface soils: Distribution patterns and mode of occurrence. *Chemosphere* **2016**, 161: 333-341.

Rodgers, R.P.; Schaub, T.M.; Marshall, A.G. Petroleomics: MS Returns to Its Roots. *Anal. Chem.* **2005**, 77: 20A-27A.

Rosenqvist, L.; Vestergren, R.; Westberg, E.; Eliaeson, K.; Norström, K.; Liljeberg, M.; Strandberg, J.; Rahmberg, M. Spridning av högfluorerade ämnen i mark från Stockholm Arlanda Airport. *Svenska miljöinstitutet* **2017**, 121.

Savory, J. J.; Kaiser, N. K.; McKenna, A. M.; Xian, F.; Blakney, G. T.; Rodgers, R. P.; Hendrickson, C. L.; Marshall, A. G., Parts-Per-Billion Fourier transform ion cyclotron resonance mass measurement accuracy with a "Walking" calibration equation. *Anal. Chem.* **2011**, 83: 1732-1736.

Schultz, M. M.; Higgins, C. P.; Huset, C. A.; Luthy, R. G.; Barofsky, D. F.; Field, J. A. Fluorochemical mass flows in a municipal wastewater treatment facility. *Environ. Sci. Technol.* **2006**, 40: 7350-7357.

Schymanski, E. L.; Jeon, J.; Gulde, R.; Fenner, K.; Ruff, M.; Singer, H. P.; Hollender, J. Identifying Small Molecules via High Resolution Mass Spectrometry: Communicating Confidence. *Environ. Sci. Technol.* **2014**, 48: 2097-2098.

Sharifan, H.; Bagheri, M.; Wang, D.; Burken, J.G.; Higgins, C.P.; Liang, Y.; Liu, J.; Schaefer, C.E.; Blotevogel, J. Fate and transport of per- and polyfluoroalkyl substances (PFASs) in the vadose zone. *Science of the Total Environment* **2021**, 771: 145427.

Smith, D.; Podgorski, D. C.; Rodgers, R. P.; Blakney, G. T.; Hendrickson, C. L. 21 Tesla FT-ICR Mass Spectrometer for Ultrahigh-Resolution Analysis of Complex Organic Mixtures. *Anal. Chem.* **2018**, *90*: 2041-2047.

Stanford, L.A.; Kim, S.; Rodgers, R.P.; Marshall, A.G. Characterization of compositional changes in vacuum gas oil distillation cuts by electrospray ionization FT-ICR mass spectrometry. *Energy & Fuels* **2006**, 20: 1664-1673.

Su, H.; Lu, Y.; Wang, P.; Shi, Y.; Li, Q.; Zhou, Y.; Johnson, A.C. Perfluoroalkyl acids (PFAAs) in indoor and outdoor dusts around a mega fluorochemical industrial park in China: implications for human exposure. *Environment International* **2016**, 94: 667-73.

Teräväinen, M.J.; Pakarinen, J.M.H.; Wickström, K.; Vainiotalo, P. Comparison of the composition of Russian and North Sea crude oils and their eight distillation fractions studied by negative-ion electrospray ionization Fourier transform ion cyclotron resonance mass spectrometry: The effect of suppression. *Energy & Fuels* **2007**, 21: 266–273.

Tokranov, A. K.; Nishizawa, N.; Amadei, C. A.; Zenobio, J. E.; Pickard, H. M.; Allen, J. G.; Vecitis, C. D.; Sunderland, E. M. How Do We Measure Poly- and Perfluoroalkyl Substances (PFASs) at the Surface of Consumer Products? *Environ. Sci. Technol. Lett.* **2019**, 6: 38-43.

Tureček, F.; McLafferty, F.W. (1993). Interpretation of mass spectra. Sausalito, CA: University Science Books. pp. 37-38. ISBN 0-935702-25-3.

USEPA. 2007. Method 1614 brominated diphenyl ethers in water soil, sediment and tissue by HRGC/HRMS.

USEPA. 2018. Assessing and Managing Chemicals under TSCA. *Fact Sheet: 2010/2015 PFOA Stewardship Program*.

van Krevelen, D.W. Graphical-Statistical Method for the Study of Structure and Reaction Processes of Coal. *Fuel* **1950**, 29: 269-284.

Wang, Z.; DeWitt, J. C.; Higgins, C. P.; Cousins, I. T. A Never Ending Story of Per- and Polyfluoroalkyl Substances (PFASs)? *Environ. Sci. Technol.* **2017**, 51: 2508-2518.

Wang, Y.; Fu, J.; Wang, T.; Liang, Y.; Pan, Y.; Cai, Y.; Jiang, G. Distribution of perfluorooctane sulfonate and other perfluorochemicals in the ambient environment around a manufacturing facility in China. *Environmental Science & Technology* **2010**, 44: 8062-8067.

Washington, J.W.; Rosal, C.G.; McCord, J.P.; Strynar, M.J.; Lindstrom, A.B.; Bergman, E.L.; Goodrow, S.M.; Tadesse, H.K.; Pilant, A.N.; Washington, B.J. Nontargeted mass-spectral detection of chloroperfluoropolyether carboxylates in New Jersey soils. *Science* **2020**, 368: 1103-1107.

Xian, F.; Hendrickson, C. L.; Blakney, G. T.; Beu, S. C.; Marshall, A. G., Automated Broadband Phase Correction of Fourier Transform Ion Cyclotron Resonance Mass Spectra. *Anal. Chem.* **2010,** 82: 8807-8812.

Yan, H.; Zhang, C.-J.; Zhou, Q.; Chen, L.; Meng, X.Z. Short-and long-chain perfluorinated acids in sewage sludge from Shanghai, China. *Chemosphere* **2012**, 88: 1300-1305.

Yan, H.; Cousins, I.T.; Zhang, C.J.; Zhou, Q. Perfluoroalkyl acids in municipal landfill leachates from China: occurrence, fate during leachate treatment and potential impact on groundwater. *Sci. Total Environ.* **2015**, 524: 23-31.

Yao, Y.; Chang, S.; Zhao, Y.; Tang, J.; Sun, H.; Xie, Z. Per-and poly-fluoroalkyl substances (PFASs) in the urban, industrial, and background atmosphere of Northeastern China coast around the Bohai Sea: Occurrence, partitioning, and seasonal variation. *Atmospheric Environment* **2017**, 167: 150-158.

Zito, P.; Podgorski, D.C.; Bartges, T.; Guillemette, F.; Roebuck Jr., J.A.; Spender, R.G.M.; Rodgers, R.P.; Tarr, M.A. Sunlight-Induced Molecular Progression of Oil into Oxidized Oil Soluble Species, Interfacial Material, and Dissolved Organic Matter. *Energy Fuels* **2020**, 34: 4721-4726.

APPENDIX A: SUPPORTING DATA

Table A 1: Percent recoveries for 24 PFASs in Fort Collins tap water and synthetic salt water (3 g/L sodium sulfate and 7 g/L sodium chloride, simulating Site C groundwater) using LLE and sequential SPE. For LLE, the percentages represent averages from three recovery experiments at PFAS concentrations of 0.1, 1, and 10 µg/L. The SPE recovery experiment was performed at 100 µg/L. PFASs were quantified on an Agilent LC/QQQ-MS. Wellington Laboratories Inc. (Guelph, ON, Canada) product MPFAC-24ES was used as internal standard at half of the spiked analyte concentration.

	Liquid-Liquid Extraction (LLE)		**Sequential Solid-Phase Extraction (SPE)**	
	Salt Water	**Tap Water**	**Salt Water**	**Tap Water**
PFBA	153	193	1828	3433
PFPeA	103	108	106	106
PFBS	98	100	101	105
4:2 FTS	137	132	72	63
PFHxA	108	105	118	115
PFPeS	96	112	82	83
PFHpA	104	108	117	115
PFHxS	99	95	82	69
6:2 FTS	106	110	120	96
PFOA	103	102	107	125
PFHpS	99	92	67	64
PFNA	96	102	68	68
PFOS	117	105	41	59
PFNS	83	104	18	2
PFDA	95	93	65	120
8:2 FTS	120	112	0	0
N-MeFOSAA	127	85	28	34
FOSA	95	93	17	37
PFDS	157	129	0	0
PFUdA	103	103	0	0
N-EtFOSAA	80	89	48	59
PFDoA	106	96	0	0
PFTrDA	118	105	0	0
PFTeDA	82	96	0	0

Table A 2: PFASs detected in the travel blank and their relative abundances.

Molecular Formula	Relative Abundance
C2H3F3O3S	0.0192
C6H6F6O2	0.0170
C5H4F6O3	0.0158
C6H4F6O3	0.0306
C4H5F5O4S	0.0887
C5H3F7O3	0.0278
C7H5F7O2	0.0237
C6H5F7O3	0.0590
C8H11F6NO2	0.0609
C6H4F8O3	0.0152
C7H7F7O4	0.3346
C8H7F7O4	0.0176
C8H5F9O2	0.0333
C6H2F10O3	0.1770
C8H5F9O3	0.0168
C10H7F9O2	0.0226
C7HF13	0.0372
C9H7F9O3	0.0781
C10H12F9NO2	0.0198
C9H7F9O4	0.0171
C8H6F10O4	0.0414
C9H7F11O2	0.0189
C7HF13O2	0.0254
C8H5F11O4	0.0592
C8H4F12O3	0.0197
C8H4F12O4	0.0191
C11H14F9NO4	0.0130
C8H2F14O2	0.0306
C10H19F5N2O5S2	0.0119
C12H23F5N2O6S2	0.0136
C10H2F18O2	0.0706
C8HF17O3S	0.0151
C13H18F9NO5S2	0.0510
C16H16F16O2	0.0163
C14H23F9N2O6S2	0.6635
C16H18F13NO6	0.0435
C12H2F22O2	0.1058
C18H18F18O2	0.0199
C16H27F9N2O8S2	0.0172
C14H2F26O2	0.0841
C17H13F23N2O	0.0419
C16H9F26O4P	0.0603
C16H2F30O2	0.1308

Table A 3: PFASs detected in the field blank and their relative abundances.

Molecular Formula	Relative Abundance
C4H2F6O2	0.0434
C5H4F6O2	0.0130
C6H6F6O2	0.1683
C5H4F6O3	0.0149
C6H4F6O3	0.0184
C6H5F7O2	0.0142
C4H5F5O4S	0.0587
C5H3F7O3	0.0427
C7H5F7O2	0.0192
C6H5F7O3	0.0621
C8H11F6NO2	0.0372
C7H7F7O4	0.2116
C8H7F7O4	0.0152
C8H5F9O2	0.0398
C6H2F10O3	0.3060
C7HF13	0.0139
C9H7F9O3	0.0687
C10H12F9NO2	0.0250
C9H7F9O4	0.0154
C10H10F10O2	0.0147
C11H9F7O3S	0.1012
C8H6F10O4	0.0370
C7HF13O2	0.0392
C8H5F11O4	0.0794
C8H4F12O3	0.0374
C8H4F12O4	0.0151
C11H14F9NO4	0.0136
C6HF13O3S	0.0134
C10H5F13O3	0.0134
C13H16F9NO4	0.0144
C8F16O3	0.0300
C9F18	0.0131
C11H13F13N2O2S	0.0227
C10H2F18O2	0.0324
C8HF17O3S	0.0461
C14H23F9N2O6S2	0.3941
C16H18F13NO6	0.0315
C25H39F13	0.0266
C12H2F22O2	0.0374
C26H41F13	0.0258
C19H31F11NO8S	0.0216
C16H21F15N2O6S2	0.0221
C14H2F26O2	0.0246
C16H9F26O4P	0.0211
C16H2F30O2	0.0321

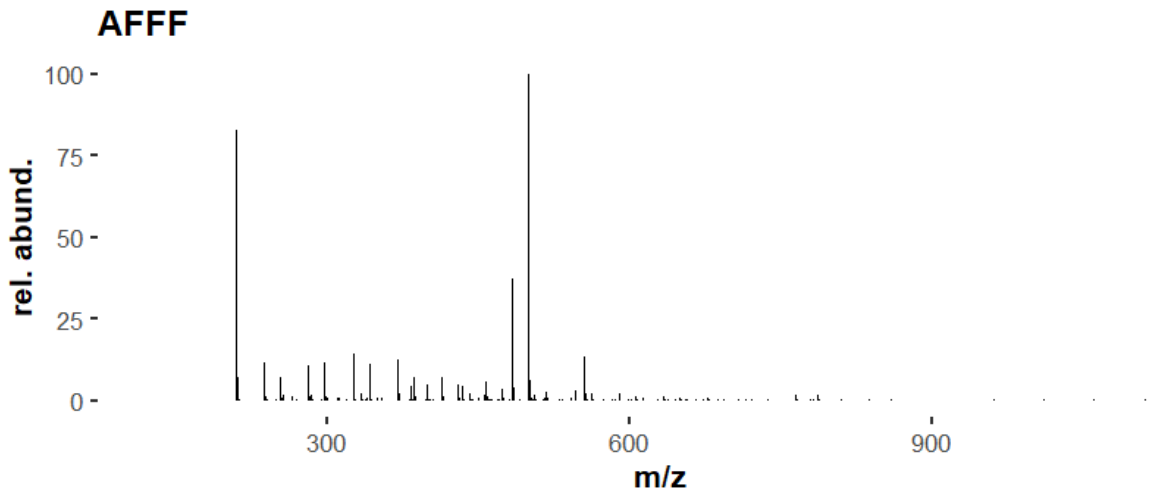

Figure A 1: FT-ICR mass spectrum for the AFFF sample.

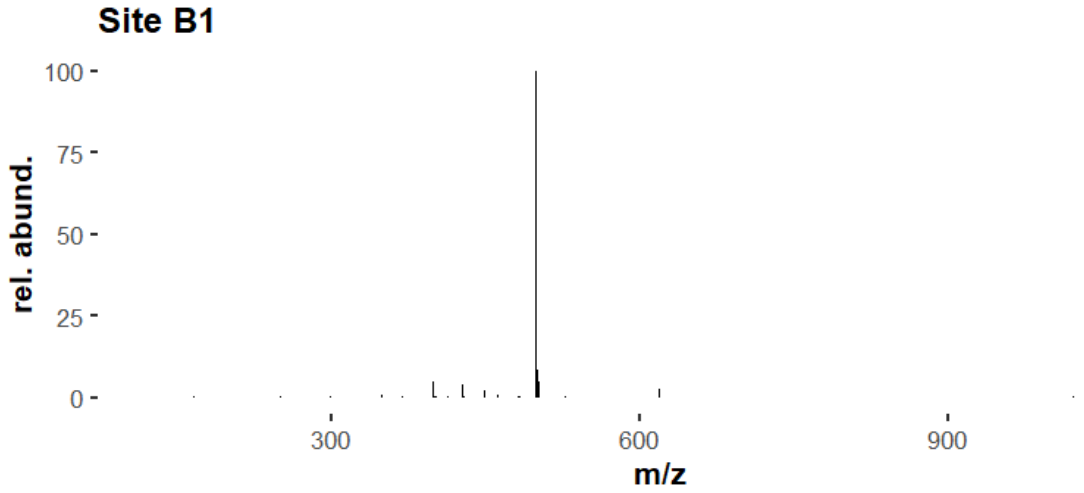

Figure A 2: FT-ICR mass spectrum for the groundwater sample from Site B 1.

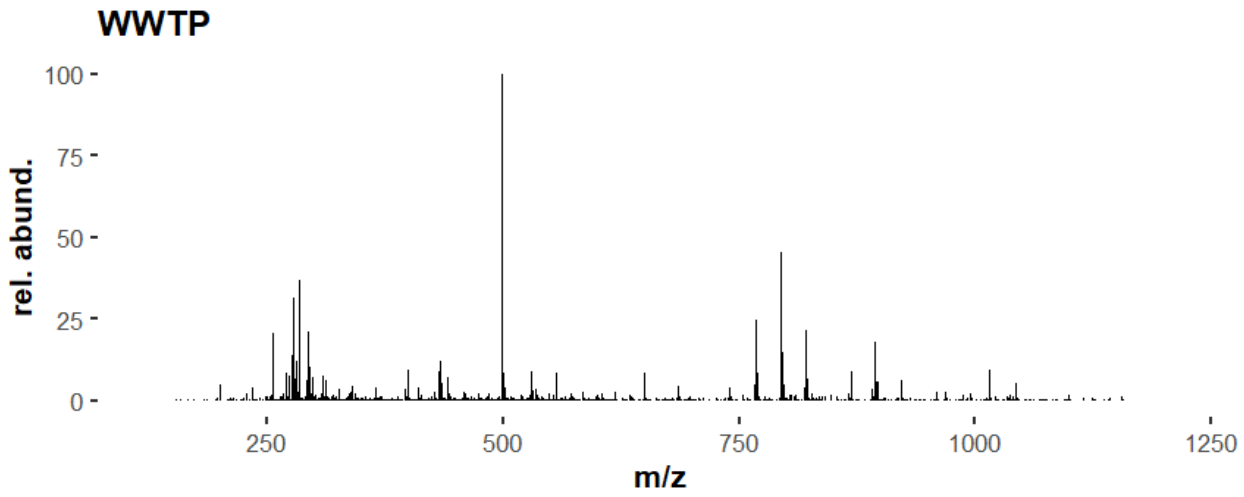

Figure A 3: FT-ICR mass spectrum for the WWTP effluent sample from Site B 1.